Submitted to Nuclear Physics

LBL-1298
Preprint c.1

STUDIES ON STATISTICALLY EXCITED SHELL MODEL NUCLEI: THE DEPENDENCE OF THE SHELL STRUCTURE AND OF THE PAIRING CORRELATION UPON ANGULAR MOMENTUM

L. G. Moretto

November 1972

Prepared for the U.S. Atomic Energy Commission
under Contract W-7405-ENG-48

For Reference

Not to be taken from this room

LAWRENCE BERKELEY LABORATORY
UNIVERSITY OF CALIFORNIA
BERKELEY

LBL-1298
c.1

DISCLAIMER

This document was prepared as an account of work sponsored by the United States Government. While this document is believed to contain correct information, neither the United States Government nor any agency thereof, nor the Regents of the University of California, nor any of their employees, makes any warranty, express or implied, or assumes any legal responsibility for the accuracy, completeness, or usefulness of any information, apparatus, product, or process disclosed, or represents that its use would not infringe privately owned rights. Reference herein to any specific commercial product, process, or service by its trade name, trademark, manufacturer, or otherwise, does not necessarily constitute or imply its endorsement, recommendation, or favoring by the United States Government or any agency thereof, or the Regents of the University of California. The views and opinions of authors expressed herein do not necessarily state or reflect those of the United States Government or any agency thereof or the Regents of the University of California.

0 0 0 0 3 8 0 0 1 0 9

STUDIES ON STATISTICALLY EXCITED SHELL MODEL NUCLEI: THE DEPENDENCE OF THE SHELL STRUCTURE AND OF THE PAIRING CORRELATION UPON ANGULAR MOMENTUM

L. G. Moretto

Department of Chemistry and
Lawrence Berkeley Laboratory
University of California
Berkeley, California 94720

November 1972

Abstract

The statistical properties of excited shell model nuclei with the inclusion of the angular momentum and the pairing correlation are studied. Particular attention is dedicated to the dependence of the shell effects and of the superfluid properties upon angular momentum. The statistical functions, generated from the pairing Hamiltonian properly generalized to account for angular momentum, are calculated for various nuclei on the basis of the Nilsson model. The neutron and proton gap parameters are evaluated as a function of temperature and angular momentum. The dependence of the critical angular momenta and of the critical temperatures upon the physical quantities characterizing the nucleus is discussed. The question of the existence of a second order phase transition associated with the disappearance of the pairing correlation is considered. The temperature scale is transformed to the excitation-energy scale and the yrast line, as well as other energy angular momentum isotherms, are calculated. The evaluation of the thermodynamical quantities for the combined system of neutrons and protons is discussed in detail. As a final product, the level densities as a function of angular momentum and excitation energy are obtained.

1. Introduction

In the past few years a substantial progress has been made in the description of the properties of excited nuclei. Level density formalisms have been developed and applied both to schematic[1-4] and realistic[5-9] single particle spectra. Such an approach has led to a quantitative understanding of the disappearance of the shell effects with increasing excitation energy.

The B.C.S. Hamiltonian has also been introduced to describe the effect of short range residual interactions in excited systems. This has been performed first for a uniform spectrum of single particle levels,[10,11] later for shell model level schemes.[12-14] In this way, the interaction of shell effects, pairing effects, and excitation energy has been studied.

Further development has led to the introduction of the nuclear deformation in conjunction with the shell model and the pairing Hamiltonian in order to describe the deformation probability of an excited nucleus.[13,14] Such a study has illustrated the disappearance of the shell structure as a function of excitation energy in a very pictorial way. An immediate application of this formalism has been made to study the stability against fission of excited superheavy nuclei and the disappearance of their fission barrier with increasing excitation energy.[15,16]

In this context it should be mentioned that the feature of the disappearance of shell effects with excitation energy contained in the statistical theories has been used to calculate the ground state shell effects as an alternative to the Strutinski method.[17-21]

In the papers mentioned so far, angular momentum has been introduced by means of the spin cut-off parameter formalism, which holds only for moderately small

values of the angular momentum. In particular, in the formalisms involving the pairing Hamiltonian, the pairing correlation was taken to be independent on angular momentum. However, angular momentum drastically affects the pairing correlation, and its effect has been accounted for in two of our previous papers.[22,23] In these papers the z projection of angular momentum was introduced as a constant of the motion by means of a Lagrange multiplier. The complete set of thermodynamical quantities was then derived for the case of an arbitrary sequence of single particle levels, assuming spherical symmetry. In order to explore the interaction of excitation energy and angular momentum with the pairing correlation without the interference of the shell effects, the formalism was applied to the uniform model, namely a model for which the single particle level spacing is a constant and where each level has a constant spin projection on the z axis. Such a simple model can be easily handled. The zero temperature angular momentum dependence of the gap parameter as well as the yrast line were calculated analytically. Furthermore the critical temperature as a function of angular momentum was shown to be a decreasing function with a rather strange anomaly at large angular momenta. In this region an antiblocking effect of temperature, called "thermally assisted pairing correlation", results in an increasing pairing correlation, or even in the onset of pairing correlation with an increase in temperature.

In the calculations mentioned above, the shell model was not included and the problem of the two components of the nucleus was not accounted for in detail. It is the purpose of the present paper to extend the discussion and the calculations to shell model nuclei where the interplay of the shell structure with pairing, angular momentum and excitation energy can be studied.

In particular, in Sec. 2 the complete statistical formalism with inclusion of pairing and angular momentum is presented; the grand partition function, the first integrals of motion like energy, particle number and total angular momentum z projection are written down explicitly as well as the gap equation, the entropy and the partial derivatives necessary for the calculation of the level density denominator.

In Sec. 3 the details of the shell model and of the B.C.S. Hamiltonian employed in the calculations are illustrated.

In Sec. 4 all the relevant statistical quantities are calculated on the basis of the shell model for each component of the nucleus and are compared with the results obtained from the uniform model. The overall dependence of the gap parameter on temperature and angular momentum is displayed. The denominator of the level density is calculated to show the discontinuity associated with the superfluid phase-transition and the existence of such a transition in actual nuclei is discussed. The entropy is displayed as a function of temperature and angular momentum, the transformation from the temperature to the energy scale is performed and the yrast line is calculated.

In Sec. 5 the neutron and proton components of the nucleus are considered at the same time, and the thermodynamical quantities, including the level density, are evaluated for the whole nucleus.

In Sec. 6 the conclusions of the work are presented, an assessment is made of the development of the statistical nuclear theories and the possible extensions and improvements of such theories are discussed.

2. Summary of the Formalism

The complete formalism describing the statistical properties of a nucleus in terms of pairing, angular momentum and excitation energy[23] is presented below. All of the quantities refer to a single nuclear component.

The logarithm of the grand partition function is:

$$\Omega = -\beta \sum (\varepsilon_k - \lambda - E_k) + \sum \ln[1 + \exp(-\beta(E_k - \gamma m_k))] + \sum \ln[1 + \exp(-\beta(E_k + \gamma m_k))] - \beta \frac{\Delta^2}{G} \quad . \quad (1)$$

In this expression ε_k and m_k are the single particle energies and spin projections respectively; β, $\alpha = \beta\lambda$ and $\mu = \beta\gamma$ are the Lagrange multipliers which fix the energy, the particle number and the angular momentum projection respectively; G is the pairing strength; Δ is the gap parameter; the quasiparticle excitation E_k is given by: $E_k = [(\varepsilon_k - \lambda)^2 + \Delta^2]^{1/2}$. The quantity β is also the reciprocal of the temperature and λ is identified with the chemical potential. The gap parameter Δ is obtained as a function of β, λ, γ by solving the gap equation:

$$\sum \frac{1}{2E_k} [\tanh \tfrac{1}{2} \beta(E_k - \gamma m_k) + \tanh \tfrac{1}{2} \beta(E_k + \gamma m_k)] = \frac{2}{G} \quad . \quad (2)$$

The constants of motion are the particle number N, the total energy E, the angular momentum projection M. These quantities are given by the following expressions:

$$N = \sum \left[1 - \frac{\varepsilon_k - \lambda}{2E_k} \left\{ \tanh \tfrac{1}{2} \beta(E_k - \gamma m_k) + \tanh \tfrac{1}{2} \beta(E_k + \gamma m_k) \right\} \right] \quad , \quad (3)$$

$$E = \sum \varepsilon_k \left[1 - \frac{\varepsilon_k - \lambda}{2E_k} \left\{ \tanh \frac{1}{2} \beta(E_k - \gamma m_k) + \tanh \frac{1}{2} \beta(E_k + \gamma m_k) \right\} \right] - \frac{\Delta^2}{G} \quad , \tag{4}$$

$$M = \sum m_k \left[\frac{1}{1 + \exp \beta(E_k - \gamma m_k)} - \frac{1}{1 + \exp \beta(E_k + \gamma m_k)} \right] \quad . \tag{5}$$

The above equations, together with the gap equation define Δ, λ, β, and γ as a function of N, E, M, G, ε_k, and m_k.

The entropy is given by:

$$S = \sum \ln[1 + \exp(-\beta(E_k - \gamma m_k))] + \sum \ln[1 + \exp(-\beta(E_k + \gamma m_k))]$$

$$+ \beta \sum \frac{E_k - \gamma m_k}{1 + \exp \beta(E_k - \gamma m_k)} + \beta \sum \frac{E_k + \gamma m_k}{1 + \exp \beta(E_k + \gamma m_k)} \quad . \tag{6}$$

The level density is given by:

$$\rho(E, N_i, M) = \frac{\exp S}{(2\pi)^{n/2} D^{1/2}} \quad . \tag{7}$$

The index i indicates that more than one component may be present (in the present case one has neutrons and protons) and n is equal to the number of Lagrange multipliers introduced in the formalism. The quantity D is given by:

$$D = \det \frac{\partial^2 \Omega}{\partial \alpha_i \partial \alpha_j} \quad , \tag{8}$$

where the α_i's indicate the Lagrange multipliers. The partial derivatives necessary for the evaluation of the determinant follow:

$$\frac{\partial^2\Omega}{\partial\mu^2} = \frac{1}{4}\sum m_k^2[\mathrm{sech}^2\,\tfrac{1}{2}\,\beta(E_k - \gamma\, m_k) + \mathrm{sech}^2\,\tfrac{1}{2}\,\beta(E_k + \gamma\, m_k)]$$

$$- \beta\Delta\,\frac{\partial\Delta}{\partial\mu}\sum\frac{m_k}{4E_k}\,[\mathrm{sech}^2\,\tfrac{1}{2}\,\beta(E_k - \gamma\, m_k) - \mathrm{sech}^2\,\tfrac{1}{2}\,\beta(E_k + \gamma\, m_k)] \tag{9}$$

$$\frac{\partial^2\Omega}{\partial\alpha^2} = \sum(\varepsilon_k - \lambda)^2\, a_k + \Delta^2\sum b_k - \beta\Delta\,\frac{\partial\Delta}{\partial\alpha}\sum(\varepsilon_k - \lambda)(a_k - b_k) \tag{10}$$

$$\frac{\partial^2\Omega}{\partial\beta^2} = \lambda\,\Delta^2\sum\varepsilon_k\, b_k + \Delta^2\sum\varepsilon_k(\varepsilon_k - \lambda)\, a_k + \sum\varepsilon_k^2(\varepsilon_k - \lambda)^2\, a_k$$

$$+ \beta\Delta\,\frac{\partial\Delta}{\partial\beta}\,[\sum\varepsilon_k(\varepsilon_k - \lambda)(a_k - b_k) + \frac{2}{\beta G}] \tag{11}$$

$$\frac{\partial^2\Omega}{\partial\mu\partial\alpha} = \frac{1}{4}\sum\frac{(\varepsilon_k - \lambda)}{E_k}\, m_k[\mathrm{sech}^2\,\tfrac{1}{2}\,\beta(E_k - \gamma\, m_k) - \mathrm{sech}^2\,\tfrac{1}{2}\,\beta(E_k + \gamma\, m_k)]$$

$$+ \beta\Delta\,\frac{\partial\Delta}{\partial\alpha}\,\frac{1}{4}\sum\frac{m_k}{E_k}\,[\mathrm{sech}^2\,\tfrac{1}{2}\,\beta(E_k + \gamma\, m_k) - \mathrm{sech}^2\,\tfrac{1}{2}\,\beta(E_k - \gamma\, m_k)] \tag{12}$$

$$\frac{\partial^2\Omega}{\partial\mu\partial\beta} = \frac{1}{4}\sum\frac{m_k}{E_k}\,\{(\varepsilon_k - \lambda)\,\varepsilon_k + \Delta^2\}[\mathrm{sech}^2\,\tfrac{1}{2}\,\beta(E_k + \gamma\, m_k) - \mathrm{sech}^2\,\tfrac{1}{2}\,\beta(E_k - \gamma\, m_k)]$$

$$+ \beta\Delta\,\frac{\partial\Delta}{\partial\beta}\sum\frac{m_k}{4E_k}\,[\mathrm{sech}^2\,\tfrac{1}{2}\,\beta(E_k + \gamma\, m_k) - \mathrm{sech}^2\,\tfrac{1}{2}\,\beta(E_k - \gamma\, m_k)] \tag{13}$$

$$\frac{\partial^2\Omega}{\partial\alpha\partial\beta} = -\,\lambda\Delta^2\sum b_k - \sum\varepsilon_k(\varepsilon_k - \lambda)^2\, a_k - \Delta^2\sum(\varepsilon_k - \lambda)\, a_k$$

$$- \beta\Delta\,\frac{\partial\Delta}{\partial\beta}\sum(\varepsilon_k - \lambda)(a_k - b_k)\quad . \tag{14}$$

The quantities a_k, b_k, $\frac{\partial\Delta}{\partial\beta}$, $\frac{\partial\Delta}{\partial\mu}$, $\frac{\partial\Delta}{\partial\alpha}$ are given by:

$$a_k = \frac{1}{4}\frac{1}{E_k^2}\left[\operatorname{sech}^2 \frac{1}{2}\beta(E_k - \gamma\, m_k) + \operatorname{sech}^2 \frac{1}{2}\beta(E_k + \gamma\, m_k)\right] , \tag{15}$$

$$b_k = \frac{1}{2\beta E_k^3}\left[\tanh \frac{1}{2}\beta(E_k - \gamma\, m_k) + \tanh \frac{1}{2}\beta(E_k + \gamma\, m_k)\right] . \tag{16}$$

$$\frac{\partial\Delta}{\partial\beta} = -\frac{\Delta^2\sum a_k + \sum a_k\,\varepsilon_k(\varepsilon_k - \lambda) - \lambda\sum b_k(\varepsilon_k - \lambda)}{\beta\Delta\sum(a_k - b_k)} \tag{17}$$

$$\frac{\partial\Delta}{\partial\mu} = -\frac{\frac{1}{4}\sum\frac{1}{E_k}\, m_k\left[\operatorname{sech}^2 \frac{1}{2}\beta(E_k + \gamma\, m_k) - \operatorname{sech}^2 \frac{1}{2}\beta(E_k - \gamma\, m_k)\right]}{\beta\Delta\sum(a_k - b_k)} \tag{18}$$

$$\frac{\partial\Delta}{\partial\alpha} = -\frac{\sum(\varepsilon_k - \lambda)(b_k - a_k)}{\beta\Delta\sum(a_k - b_k)} . \tag{19}$$

The above three derivatives are to be set equal to zero when $\Delta = 0$.

3. The Shell Model and the Pairing Hamiltonian

3.1. THE SHELL MODEL

A most convenient model for its simplicity and its ability to account for the experimental shell structure is the Nilsson model. The version of the Nilsson model used here is that described by Nilsson et al.[24] The parameters which characterize the model are the oscillator quantum $\hbar\omega_o$, the spin orbit parameter κ and the ℓ^2 parameter $\kappa\mu$. The values of κ and μ have been taken from ref. 24 and for the oscillator quantum the following isospin dependent expression has been used:

$$\hbar\overset{o}{\omega}_N = \hbar\overset{o}{\omega}_o(1 + 1/3\,\frac{N-Z}{A}) \qquad , \quad \hbar\overset{o}{\omega}_o = 41\,A^{-1/3} \tag{20}$$

$$\hbar\overset{o}{\omega}_p = \hbar\overset{o}{\omega}_o(1 - 1/3\,\frac{N-Z}{A})$$

3.2. THE PAIRING HAMILTONIAN

The residual interaction, in the pairing approximation, takes the general form:

$$H_{Pairing} = -\sum_{kk'} G_{kk'}\, a^{\dagger}_{\bar{k}'}\, a^{\dagger}_{k}\, a_{k}\, a_{\bar{k}} \quad , \tag{21}$$

where the $a^{\dagger}_k$ a_k are the single particle creation and annihilation operators and $G_{kk'}$ are the pairing matrix elements of the short range residual interaction. In the present paper it is assumed that all of the pairing matrix elements are equal to a constant G. Unfortunately with such an approximation the gap equation diverges. It is therefore necessary to truncate the sum in the gap equation and in the related expressions by means of a lower and upper bound in order to insure convergence. This is not a bad approximation because, due to the Pauli principle,

the residual interaction affects the system close to the Fermi surface only. As discussed in ref. 24, the following expression gives adequate values for G:

$$G \times A = g_o \pm g_1 \frac{N-Z}{A} \quad , \quad g_o = 19.2 \text{ MeV}, \quad g_1 = 7.4 \text{ MeV} \tag{22}$$

provided that the lower and upper bound for the summation be taken $\sqrt{15N}$ or $\sqrt{15Z}$ levels above and below the Fermi surface. The plus sign refer to protons and the minus sign refers to neutrons. This prescription fulfills two purposes: a) it reproduces the experimental trend for the even-odd mass differences, $\Delta \sim 12/A^{1/2}$; b) for the nuclei in which we are interested, namely for $A > 140$ the energy interval about the Fermi surface is quite large and it does not pose any serious problem concerning the possible overflowing of quasi-particles beyond the bounds even at the largest temperatures of interest. The above prescription fails for Z or N less than 60 for lack of a sufficient number of levels below the Fermi surface and may fail in finite potentials of the Wood-Saxon type due to an insufficient number of bound levels above the Fermi surface. In such cases it is necessary to reduce the summation range and to renormalize the pairing strength accordingly.

4. Shell Model Calculations with One Component

In the formalism illustrated in Sec. 2, only the z component M of the total angular momentum is accounted for, while no explicit mention is made about the total angular momentum I. However, for a spherically symmetric system, the formalism is indeed complete. Because of such a symmetry, the laboratory fixed z axis can be made to coincide with the body fixed z' axis and both can be aligned within the quantum mechanical uncertainty with the angular momentum direction. In this case the whole physical effects of the angular momentum are taken up by the z projection and it is possible to identify and substitute M with I. This is correct in the classical limit; in the quantum mechanical limit the substitution should be $M \rightarrow \sqrt{I(I+1)} \sim I + \frac{1}{2}$.

4.1 DEPENDENCE OF Δ UPON ANGULAR MOMENTUM AT T = 0

The angular momentum is generated by breaking pairs and by aligning the resulting quasiparticles, and it tends to destroy the pairing correlation through the blocking of the single particle levels close to the Fermi surface. In the case of the uniform model, a simple and elegant relationship between Δ and I for T = 0 is obtained:

$$\Delta = \Delta_o \left(1 - \frac{I}{I_{cr}}\right)^{1/2} \tag{23}$$

where Δ_o is the gap parameter for I = 0, T = 0 and I_{cr} is given by:

$$I_{cr} = g\, m\Delta_o \quad . \tag{24}$$

In this equation, g is the density of the doubly degenerate single particle levels and m is the single particle spin projection on the z axis taken to be

the same for all the levels. These expressions illustrate the decrease in the pairing correlation with increasing angular momentum and its sudden disappearance at the critical angular momentum I_{cr}. The dependence of I_{cr} on the physical parameters of the uniform model can be used as a guide to understand the general trends observed in actual shell model calculations.

In the case of a shell model level scheme, the calculation is more complicated because of the discontinuities which appear in the relevant equations for $\beta = \infty$ or $T = 0$. However one can gain a sufficiently accurate picture by setting β equal to a very large value. The desired function can be obtained by solving a system of three non linear equations: the gap equation (2) the angular momentum equation (5) and the particle equation (3). Once β is assigned the chosen value, the system can be solved for Δ, γ, and λ. Such a system can be solved by iteration after linearization in the neighborhood of a guess. The calculation can be simplified by solving the gap equation (2) and the particle equation (3) for a fixed value of γ; the solution for Δ and λ can be introduced in the angular momentum equation (5) together with γ to obtain $M \equiv I$. In fig. 1 the results are shown for the neutron and proton components of ^{194}Pt. It should be made clear that the angular momentum in abscissa refers to a single component only and not to the total nucleus. It can be noticed that the critical angular momentum for the neutron component is approximately twice that of the proton component. This is mainly a consequence of the smooth dependence of I_{cr} on the single particle level density g, on the gap parameter Δ_o and on the average spin projection m, as illustrated by the equation (24). The overall dependence of Δ on I is also rather close to that predicted by equation (23). However, the shell structure

affects such a dependence substantially. For instance, the proton gap parameter becomes double-valued at angular momenta close to the critical value. A check on the total energy of the system corresponding to the two values of Δ indicates that the energy is the same. This means that, at these angular momenta, the nucleus can be indifferently paired or unpaired without change in energy.

4.2. DEPENDENCE OF THE CRITICAL TEMPERATURE UPON ANGULAR MOMENTUM

The present formalism predicts that, at zero angular momentum, the pairing correlation decreases with increasing temperature and vanishes at a critical temperature T_{cr}. In the case of the uniform model, the critical temperature has the value:

$$T_{cr} = 2\Delta_o/3.50 \quad . \tag{25}$$

The angular momentum also tends to decrease the pairing correlation as seen in the previous section. Therefore the critical temperature is expected to decrease with increasing angular momentum.

The dependence of the critical temperature upon angular momentum for the uniform model is shown in fig. 2. The expected dependence is indeed observed; however, for angular momenta close to the critical value, the critical temperature becomes double-valued. It appears that, for angular momenta slightly above the critical value, an increase in temperature brings the pairing correlation back. Such phenomenon, described in our previous paper[23] as "thermally assisted pairing correlation" has the following explanation. The blocking produced by quasi-particles is most effective when it occurs close to the Fermi surface. At large angular momenta and for T = 0 the effect of blocking is maximum because all the quasiparticles are tightly packed

around the Fermi surface. An initial increase of the temperature, instead of breaking pairs, actually spreads out the quasiparticles, thus diminishing the effect of blocking.

In order to calculate the angular momentum dependence of the critical temperature for a shell model nucleus one can proceed as follows. The gap equation (2) and the particle equation (3) can be solved simultaneously for λ_{cr} and γ_{cr} after setting $\Delta = 0$ and T equal to one of the successive values between 0 and the critical temperature at zero angular momentum. The angular momentum can be obtained from equation (5) by setting $\Delta = 0$ and by introducing T, γ_{cr}, and λ_{cr}. In this way it is possible to solve the problem avoiding the system of three non linear equations which should be dealt with in principle.

In fig. 3 some examples of calculations are presented. The neutron critical temperatures shown in fig. 3b have been chosen in order to illustrate the effect of the N = 126 shell. As N approaches 126, both the critical temperature and the critical angular momentum are seen to decrease regularly. This reflects mainly the local decrease in single particle level density. The "thermally assisted pairing correlation" is to a large extent masked by the local spin fluctuations. The neutron critical angular momenta are in general much larger than the proton critical angular momenta because of the much larger average single particle level density. The proton critical temperatures shown in fig. 3a have been chosen to illustrate the effect of a high spin state. While the Z = 78 and Z = 80 curves show a regular decrease in the critical temperature and in the critical angular momentum due to the Z = 82 shell, the Z = 86 curve shows a moderate increase in the critical angular

momentum. This is mainly due to a high spin level ($h_{9/2}$) which provides a considerable average quasi-particle contribution to the total angular momentum.

4.3. THE GAP PARAMETER AS A FUNCTION OF T AND I

The complete dependence of Δ upon T and I for the uniform model can be observed in fig. 4. The presence of the "thermally assisted pairing correlation" can be best seen for angular momenta close to the critical value. In the shell model case, the calculation of the lines of equal Δ can be performed in the simplest way as illustrated in subsec. 4.2. Instead of setting $\Delta = 0$, Δ is set equal to the desired value, the value of T is chosen among those of a suitable grid and eq. (2) and eq. (3) are solved for γ and λ. The values of Δ, T, γ, and λ are then substituted in eq. (5) and the corresponding value of the angular momentum is obtained. In fig. 5 the Δ surfaces are presented in the form of isometric projections for the neutron and proton components of various nuclei. Again it can be observed that the shell structure affects both the qualitative and quantitative features of the Δ surface rather dramatically. The Δ surface extends towards large values of T for nuclei with large single particle level density at the Fermi surface, it extends toward large angular momentum values for nuclei with large j values close to the Fermi surface.

Beneath the apparent simplicity of these results, a very complicated behaviour of the system can be observed. As examples of the complex anatomy of the nuclear structure, the dependences of γ on I, of Δ on γ and of λ on Δ at various temperatures for the proton component of $^{220}_{86}Rn$ are shown in figs. 6, 7, and 8. These functions vary quite substantially from one nucleus

to another and contain all of the thermodynamical information concerning the nuclear properties.

The calculations become rather difficult at very low temperatures: this is due to the fact that the multidimensional surfaces represented by eq. (2) and (5) become very ill-behaved at low T and tend to become discontinuous for T = 0. Because of this, the linearization of the various systems of equations necessary for the numerical search of the solution becomes problemetic. The quantities β, γ, and λ may even lose their monotonic dependence on energy, angular momentum, and particle number, respectively. Furthermore, the saddle point method which underlies the whole formalism described here, tends to fail at very low temperatures.

4.4. THE SUPERCONDUCTIVE PHASE TRANSITION AND THE DISCONTINUITY IN THE SPECIFIC HEAT

The line of the critical temperature in the T, I plane represents the locus of the points at which Δ reaches zero, the superfluid and superconductive properties of the system disappear, and the nucleus reverts to a system of uncorrelated nucleons. At this point the residual interaction affects the properties of the system only through a shift of the ground state energy: namely the nucleus, excited above the critical temperature, behaves as if its ground state was unpaired instead of paired.

The transition from the paired to the unpaired region can be induced either by increasing the temperature at constant angular momentum, or by increasing the angular momentum at constant temperature. Such a phase transition is of the second order, namely a discontinuity is observed in the specific heat instead of appearing in the free energy. In the present formalism, the

determinant which appears in the expression for the level density is a monotonic function of the specific heat and indeed presents the expected discontinuity. In fig. 9 the determinant for the uniform model is presented as a function of temperature for different angular momenta. In fig. 10 two examples of calculations on the basis of the shell model are presented. In these pictures the determinant is expressed as a function of angular momentum for different temperatures.

In all of these pictures the discontinuity is clearly visible both when the critical line is crossed by increasing the temperature and by increasing the angular momentum. In the case of the uniform model, the determinant is independent of angular momentum outside the critical region. Due to the shell structure such independence is not verified in shell model nuclei as can be seen by the fact that the lines of specific heat at constant temperatures are not horizontal outside the critical region.

A note of caution should be made concerning the real existence of such discontinuities in actual nuclei. In the present formalism the gap parameter Δ is chosen in such a way as to maximize the grand partition function e^{Ω}, namely be requiring that $\frac{\partial \Omega}{\partial \Delta} = 0$. It is easily seen that such a condition is equivalent to the gap equation. In a macroscopic system the probability distribution in Δ is infinitely sharp, so that its most probable value contains all the necessary information regarding the system. In particular, at the temperature for which the most probable value of Δ goes to zero, the whole distribution goes to zero and a discontinuity appears. For small systems, like a nucleus, the width and the higher moments of the Δ distribution become important.[25] In fig. 11, the probability distribution in

Δ for the uniform model is presented for various temperatures at zero angular momentum. The width of the distribution appears to be always comparable with the most probable value. Furthermore, as the temperature increases, the asymmetry of the distribution becomes so substantial as to make the average and most probable values of Δ quite different. While, at the critical temperature and above, the most probable value of Δ vanishes, the average value of Δ remains finite. Because of the fluctuations just described, no discontinuity is expected to appear at the critical temperature. In fig. 12 the specific heat of the system is shown both for the case in which the most probable value of Δ is used and for the case in which the average value is employed. In the latter more realistic case, the discontinuity is smoothed out over a rather large temperature interval. As a conclusion, no discontinuity should exist in the case of nuclei but a smooth though rather rapid transition from a correlated to an uncorrelated phase is to be expected. We shall continue using the present formalism which allows for a phase transition because of its greater simplicity and power. However, one should be cautious in taking seriously any conclusion which depends directly upon the quantitative use of the gap equation or upon the presence of a phase transition.

4.5. THE ENTROPY AS A FUNCTION OF ANGULAR MOMENTUM AND TEMPERATURE

The behaviour of entropy as a function of angular momentum for different temperatures in the case of the uniform model is shown in fig. 13. In the region where the pairing correlation is absent, the entropy at a fixed temperature does not depend upon angular momentum. In the region where pairing is present, the dependence of entropy upon angular momentum is substantial because

of the strong effect of the angular momentum upon the gap parameter. A similar calculation performed for a shell model nucleus, is shown in fig. 14. While the shell structure is seen to modify the general picture in a quantitative way, the qualitative features are retained, especially at sufficiently large temperature. In these latter examples the entropy is clearly affected by the onset of pairing at small angular momentum. However, even at angular momenta larger than the critical value the entropy is not completely independent on angular momentum. This is due to the non uniform distribution in spin projections and spacings in the shell model scheme.

4.6. CHANGE TO THE ENERGY SCALE

The excitation energy, more than the temperature, is the most suitable independent variable for the presentation of the various quantities. In order to achieve such a transformation, it is sufficient to express the excitation energy in terms of temperature and angular momentum. A most interesting quantity is the energy vs. angular momentum isotherm for T = 0. Such a function is usually called yrast line and represents the locus of the states with largest angular momentum at fixed energy or of the states of lowest energy at fixed angular momentum. For the uniform model such a function can be written down in closed form:[22-23]

$$E_{yrast} = \begin{cases} \frac{1}{2} g \Delta_o^2 \frac{I}{I_{cr}} \left(2 - \frac{I}{2I_{cr}}\right) & \text{for } I \leqslant I_{cr} \\ \frac{1}{2} g \Delta_o^2 + \frac{I^2}{4m^2 g} & \text{for } I \geqslant I_{cr} \end{cases} \tag{26}$$

Above the critical angular momentum the yrast line is a parabola typical of a

rotating rigid body with moment of inertia $\mathcal{J}_R = 2m^2 g$. Also it is apparent that the effect of the pairing correlation is completely absorbed into an energy shift equal to the condensation energy $C = \frac{1}{2} g \Delta_o^2$. The above equations show that, along the yrast line, the transition from paired to unpaired systems occurs at an energy:

$$E_{cr} = \frac{3}{4} g \Delta_o^2 = \frac{3}{2} C \quad . \tag{27}$$

Below the critical angular momentum, the yrast line is also a parabola, with negative second derivative (fig. 15). In the same figure, other energy angular momentum isotherms for T > 0 are also shown.

It is instructive to calculate the moment of inertia and the angular frequency along the yrast line in the paired region by means of eq. 26. The angular frequency is given by:

$$\omega = \frac{\partial E}{\partial I} \quad , \tag{28}$$

where the partial derivative is taken by keeping constant any parameter affecting the shape or the internal structure of the system. In the present case, as in any case where the parameters are allowed to attain their equilibrium value, we have:

$$\omega = \frac{dE}{dI} = \frac{\partial E}{\partial I}\Big|_{\Delta} + \frac{\partial E}{\partial \Delta}\Big|_{G} \frac{d\Delta}{dI} \quad . \tag{29}$$

The partial derivative of E with respect to Δ at constant pairing strength G is equal to zero because the value of the gap parameter Δ is determined in such a way as to minimize the total energy, or, in the case of T > 0, the free

energy. Also, it is easy to show that the Lagrange multiplier γ represents the angular velocity of the system at any temperature and coincides with ω at $T = 0$. The moment of inertia is given by:

$$\mathcal{J} = \frac{I}{\omega} \tag{30}$$

By means of eq. 26 one obtains the very simple expressions:

$$\omega = \frac{2I_{cr}}{\mathcal{J}_R}\left(1 - \frac{I}{2I_{cr}}\right) \tag{31}$$

$$\mathcal{J} = \mathcal{J}_R \frac{I/I_{cr}}{2-I/I_{cr}} \quad . \tag{32}$$

As the angular momentum increases from 0 to I_{cr}, the moment of inertia increases from zero to its rigid value. At the same time the angular frequency <u>decreases</u> from the value $\frac{2I_{cr}}{\mathcal{J}_R}$ to the value $\frac{I_{cr}}{\mathcal{J}_R}$. Above the critical temperature the moment of inertia remains constant and equal to its rigid value, while the angular frequency <u>increases</u> as in the expression $\omega = \frac{I}{\mathcal{J}_R}$.

It follows that even this very crude model predicts a "back-bending" in the now fashionable plot of the moment of inertia versus the square of the angular frequency. In general a back-bending is observed whenever $\frac{d^2E_{yrast}}{dI^2} < 0$.

For a shell model nucleus, the evaluation of the yrast line is more complicated, again because of the discontinuities which appear for $T = 0$. Still by setting $\beta = \frac{1}{T}$ equal to a large number and solving the proper set of equations for Δ, λ, γ, one can calculate an isotherm which is as close as

desired to the T = 0 isotherm. Examples of such curves, together with higher isotherms are shown in fig. 16. At sufficiently large temperature and angular momentum the isotherms are approximately parabolic. Smooth deviations from the parabolic behaviour are due to shell effects which introduce fluctuations in the moment of inertia. Below the critical temperature and the critical angular momentum, the pairing effects dominate the picture. However, a comparison between fig. 15 and fig. 16 shows that the yrast line has a negative second derivative in the case of the uniform model, while it has zero or positive second derivative in the case of the proton and neutron components of $^{194}_{78}$Pr. The reason for such a difference is related to the very different spin projection distributions in the two cases, a δ function in the former case, and an approximately constant distribution with a sharp cut off in the latter case.

5. Shell Model Calculations with Two Components

5.1. THE MATCHING OF THE NEUTRON AND PROTON COMPONENTS

In order to describe the overall statistical properties of a nucleus, both components, neutrons and protons, must be simultaneously accounted for. This presents the problem of finding the contribution of the neutron and proton components to the various thermodynamical quantities for a nucleus with fixed excitation energy and fixed angular momentum projection. The answer is contained in the statistical mechanics formalism. While the number of particles of each component is specified by means of two Lagrange multipliers α_N and α_P, the total energy and the total angular momentum projection are specified by means of a single Lagrange multiplier for each quantity, β for the energy and μ for the angular momentum. The thermodynamical quantities Ω, E, S, M, are additive: therefore the proper solution is obtained by writing:

$$\Omega = \Omega_N + \Omega_P; \qquad E = E_N + E_P; \qquad M = M_N + M_P \tag{33}$$

where each of the components is characterized by the same β and the same μ or by the same T and the same γ.

In principle the solution of the statistical problem involves the simultaneous solution of six non linear equations in the six unknown: α_N, α_P, β, μ, Δ_N, Δ_P. The equations are: two particle equations, two gap equations, one energy equation and one angular momentum equation. In other words, given the neutron and proton numbers N, Z, the total energy E, the total angular momentum projection M and the neutron and proton pairing strengths G_N, G_P, one can solve for the two chemical potentials λ_N, λ_P, for the two gap parameters Δ_N, Δ_P, for the temperature $T = \frac{1}{\beta}$ and for γ (or μ). Once these quantities

have been calculated, all the statistical functions can be evaluated. It is useful to realize that the neutron and proton components are coupled only by the energy and angular momentum equations. Furthermore, for sufficiently large energy and/or angular momentum the pairing correlation vanishes thus reducing by two the dimensionality of the problem. These considerations suggest that it is possible to simplify the numerical solution of the problem by considering the two components one at a time. The simplest case arises when pairing is absent. In this case one can generate a suitable grid in β and γ. At each point of the grid the particle equations both for neutrons and protons can be solved independently for λ_N and λ_P. The quantities β, γ, λ_N, and λ_P are then used to evaluate E, M, and S. In order to obtain the thermodynamical functions in terms of a regular grid in E and M (or I) a simple two dimensional interpolation scheme can be used.

A more complicated case arises in the paired region. Again it may be useful to set up a γ, β grid at each point of which two independent sets of two non linear equations (the gap equation and the particle equation) must be simultaneously solved for Δ and λ for both kinds of particles. Again one can calculate all the thermodynamical quantities and express them in terms of a regular grid in E and M by means of interpolation. A possible alternative to the above described mode of operation is that of calculating $\gamma = \gamma(\beta)$ for a fixed temperature grid at Δ = constant. The advantage of such a procedure is that of obtaining iso-Δ lines without interpolation. However such a procedure involves the serious difficulty of matching γ's at constant temperature between the two components.

The match of the two nuclear components is best observed in fig. 17. In this figure the level density denominator is shown as a function of angular momentum for various temperatures. The presence of the two components is made evident by the two discontinuities associated with the neutron and proton phase transitions.

In fig. 18 the total entropies of three nuclei, $^{194}_{78}Pt$, $^{198}_{80}Hg$, and $^{220}_{86}Rn$ are shown as a function of temperature and total angular momentum. Together with the lines of constant entropy the figures also show the neutron and proton critical temperatures vs. angular momentum. In this kind of presentation, the uniform model without pairing is characterized by horizontal equidistant straight lines. The effect of pairing in the above nuclei at zero angular momentum is visible in the compression of the lower isoentropy lines towards the critical temperatures. As the angular momentum increases the compression is less pronounced, due to the decrease of the pairing correlation. At low angular momenta the neutron critical temperature is above the proton critical temperature. The situation is reversed at higher angular momentum with the consequence that the proton correlation is the last to disappear, even though the critical angular momenta for the proton components are in general smaller than the critical angular momenta for the neutron components.

In fig. 19 the total entropies for the same nuclei are presented as a function of excitation energy and angular momentum. The lower line in each figure corresponds to T = 0 and represents the yrast line for the whole nucleus. From its deviation from a parabola one can learn about the perturbations introduced by the shell and pairing effects. The lines indicating the disappearance of the pairing effects for both neutrons and protons are also shown.

In the case of the uniform model, the lines of constant entropy are parabolae. The actual isoentropy line do in fact approach a parabolic behavior at large temperatures and angular momenta where the pairing and shell effects have been washed out.

5.2. FINAL EVALUATION OF THE LEVEL DENSITIES

At the beginning of Sec. 4 it was shown that the formalism could account completely for the total angular momentum I, although only the z projection M was introduced explicitly. In the case of spherical symmetry this is accomplished by substituting M with I in all the functions expressing intrinsic properties of the nucleus. However, in the evaluation of the level densities one has to account for the statistical factor associated with angular momentum. In order to determine such an effect we use the procedure suggested by Bethe:[26]

$$\rho(E, I) = \rho(E, M) - \rho(E, M+1) \quad , \tag{34}$$

or, with good approximation

$$\rho(E, I) = - \frac{d}{dM} \rho(E, M)\Big|_{M = I + 1/2} \quad . \tag{35}$$

In order to evaluate such a derivative one can write approximately:

$$\rho(E, M) \simeq f(E, I) e^{-M^2/2\sigma^2} \quad , \tag{36}$$

where

$$\sigma^2 = \frac{I}{\beta\gamma} \tag{37}$$

In such an expression f(E, I) and σ^2 depend on I through the quantities which describe the intrinsic nuclear properties. The derivative can now be taken

$$\rho(E, I) = \frac{2I + 1}{2\sigma^2} f(E, I)\, e^{-(I + \frac{1}{2})^2/2\sigma^2} \tag{38}$$

$$= \frac{2I + 1}{2\sigma^2} \rho(E, M = I + 1/2) \quad . \tag{39}$$

Such an approximation permits a straightforward evaluation of the total level density. In fig. 20 the natural logarithms of the level densities for $^{194}_{78}Pt$, $^{198}_{80}Hg$, and $^{220}_{86}Rn$ are presented as a function of energy and angular momentum. The resemblence with fig. 19 is, of course, very close. The main difference is related to the factor (2I + 1) in eq. (39) and is particularly visible in the upsweep of the lines of equal level densities close to zero angular momentum.

6. Conclusions

In the preceding sections it has been shown how it is possible to include a substantial amount of physics in the calculation of the statistical nuclear properties. The shell model has been used in the formalism as well as a short range residual interaction in the form of the pairing approximation. The angular momentum has been introduced in a consistent way as an additional constant of motion. Certainly this kind of calculation represents an improvement over the old level density expressions which cannot be considered more than gross interpolation formulae. The wealth of details obtained in the present calculation allows one to follow the evolution of the system as the excitation energy and the angular momentum increase. In fact, this formalism provides the user with a comprehensive view of a large number of physical quantities like the pairing gap, the moment of inertia, the rotational frequency, the entropy and so on.

However, limitations of various nature are inherent to the model. A minor limitation is associated with the use of the saddle point approximation which results in the fact that the constants of motion are not held rigorously constant but are constant only on the average. However, this defect is not serious except at the very lowest temperatures where the fluctuations are exceedingly large and the saddle point method itself fails. A somewhat more serious difficulty, very much related to the previous ones, has to do with the spurious prediction of sharp phase transitions as the system undergoes a change from the paired to the normal configuration.

The shortcomings discussed so far are related to the statistical approach. Serious difficulties are associated with the total Hamiltonian as

well. The single particle part of the Hamiltonian used in the present formalism is not self-consistent. In the Hartree-Fock spirit, each configuration should be characterized by its own self-consistent single particle spectrum. It is practically imposible to achieve such a kind of self-consistency in a statistical calculation performed within the microcanonical ensemble. In the grand canonical sense, by using the thermal averages of the occupation numbers, it may be possible to incorporate a Hartree-Fock self consistency in the future. For the moment the experimental existence of sharp shell effects in the density of neutron resonances substantiates the hope that the single particle spectrum associated with the ground state may not be a totally inaccurate representation of the single particle spectrum in excited nuclei.

The residual interaction used in the present calculation is rather schematic and can be improved. It is possible, for instance, to use the actual matrix elements of a short range attractive force instead of using a constant pairing strength as in the present paper and, in fact, such a kind of calculation is in progress. However, the elimination of the pairing approximation which only considers the scattering of pairs of particles in time reversed orbitals does not seem very easy to achieve at the moment. Methods more directly related to the spectroscopical calculations may be more effective in properly handling very complicated residual interactions.

A final comment should be made concerning the possibility of accurately reproducing experimental data. It should be possible to reproduce the level densities, or other related properties, at sufficiently large excitation energies, say above 10 MeV, rather accurately with minor adjustments of the parameters of the model. Unfortunately, the main amount of information comes from neutron

resonances, usually at excitation energies smaller than 7 MeV. At these energies any small inadequacy of the shell model or of the residual interaction will produce very large deviations in the level densities. Therefore, the ambitious project of accurately reproducing level densities in this region may still require substantial improvement in the Hamiltonian used in the calculation. Still one may hope that the present formalism will be of help in reproducing the qualitative and semi-qualitative features of the landscape of excited nuclei and in giving guidance for the understanding of experimental information.

Acknowledgments

The author wishes to thank Mr. T. Clements for his constant and invaluable help with the numerical calculations, and Dr. S. G. Thompson for his encouragement and assistance.

References

1) N. Rosenzweigh, Phys. Rev. 105 (1957) p. 50; ibid 108 (1957) 817

2) P. B. Kahn and N. Rosenzweigh, Phys. Rev. 187 (1969) 1193

3) A. Gilbert, Lawrence Radiation Laboratory Report, UCRL-18095 (1968)

4) H. Baba, Nucl. Phys. A159 (1970) 625

5) M. Hillman and J. R. Grover, Phys. Rev. 185 (1969) 1303

6) F. C. Williams, Nucl. Phys. A133 (1968) 33

7) L. G. Moretto, R. Stella, V. Caramella-Crespi, Energia Nucleare 17 (1970) 436

8) V. S. Ramamurthy, S. S. Kapoor, S. K. Kataria, Phys. Rev. Letters 25 (1970) 386

9) F. C. Williams, G. Chan, J. R. Huizenga, Nucl. Phys. A187 (1972) 225

10) M. Sano and S. Yamasaki, Prof. Theor. Phys. 29 (1963) 317

11) D. W. Lang, Nucl. Phys. 42 (1963) 353

12) P. Decowski, W. Grochulski, A. Marcinkowski, K. Siwek, Z. Wilhelmi, Nucl. Phys. A110 (1968) 129

13) L. G. Moretto and R. Stella, Phys. Letters 32B (1970) 558

14) L. G. Moretto, Nucl. Phys. A182 (1972) 641

15) L. G. Moretto, Phys. Letters 34B (1971) 191

16) L. G. Moretto, Nucl. Phys. A180 (1972) 337

17) V. S. Ramamurthy, S. S. Kapoor, and S. K. Kataria, Phys. Rev. Letters 25 (1970) 386

18) L. G. Moretto, Phys. Letters 38B (1972) 393

19) F. C. Williams, G. Chan, J. R. Huizenga, Nucl. Phys. A187 (1972) 225

20) R. Bengtsson, Nucl. Phys. A198 (1972) 591

21) A. Jensen and J. Damgaard, preprint

22) L. G. Moretto, Phys. Letters 35B (1971) 379

23) L. G. Moretto, Nucl. Phys. A185 (1972) 145

24) S. G. Nilsson, C. F. Tsang, A. Sobiczewski, Z. Szymanski, S. Wychech, G. Gustafson, I. L. Lamm, P. Moeller and B. Nilsson, Nucl. Phys. A131 (1969) 1

25) L. G. Moretto, Phys. Letters 40B (1972) 1

26) H. Bethe, Phys. Rev. 50 (1936) 332; ibid. 53 (1938) 675

Figure Captions

Fig. 1. Gap parameter Δ as a function of angular momentum for the neutron and proton components of ^{194}Pt at a temperature value approaching zero. The angular momentum refers to a single component and not to the whole nucleus.

Fig. 2. Dependence of the critical temperature upon angular momentum for the uniform model.

Fig. 3. Dependence of the critical temperature upon angular momentum for the proton a) and neutron b) components of various isotopes. Notice the decrease in T_{cr} and I_{cr} as the N = 126 shell is approached. A large increase in I_{cr}, associated with the proton $h_{9/2}$ level is also seen for Z = 86.

Fig. 4. Contour map of the gap parameter as a function of temperature and angular momentum for the uniform model. The lines of constant gap parameter are spaced 0.05 Δ_o from $\Delta/\Delta_o = 1.0$ to $\Delta/\Delta_o = 0.1$. The outer line corresponds to $\Delta/\Delta_o = 0$.

Fig. 5. Isometric projections of the gap parameter as a function of temperature and angular momentum for the proton and neutron components of $^{194}_{78}Pt$ a,b) $^{198}_{80}Hg$ c,d) and $^{220}_{86}Rn$ e,f).

Fig. 6. Dependence of γ upon angular momentum at various temperatures for the proton component of $^{220}_{86}Rn$. The effect of pairing is evident at the lowest temperatures where γ depends rather weakly on angular momentum. At the highest temperatures the linear dependence typical of a body rotating with a constant moment of inertia is observed.

Fig. 7. Gap parameter Δ as a function of γ at various temperatures for the proton component of $^{220}_{86}Rn$.

Fig. 8. Dependence of the chemical potential λ upon Δ at various temperatures for the proton component of $^{220}_{86}Rn$. At the lowest temperature λ shows strong variations associated to the discreteness of the single particle levels. As the temperature increases the shell structure is washed out and peculiar longer range trends are observed.

Fig. 9. Square root of the determinant (eq. 8) as a function of temperature and angular momentum for the uniform model. The lowest line corresponds to $I/I_{cr} = 0$ and the following lines are spaced at intervals equal to $I_{cr}/7$. The energy unit is equal to the pairing condensation energy and equal to twice the rotational energy at $I = I_{cr}$.

Fig. 10. Square root of the denominator (in MeV) as a function of temperature and angular momentum for the proton a) and neutron b) components of $^{194}_{78}Pt$. Notice the discontinuities associated with the phase transition and some sharp fluctuations occuring in a) at the lowest temperatures due to peculiarities in the shell structure.

Fig. 11. Probability distribution of the gap parameter Δ at various temperatures. The values of Δ at the maxima of the distributions correspond to the values obtained by solving the gap equation. The uniform model used in the calculation is characterized by $g = 7\ MeV^{-1}$ and $\Delta_o = 1$ MeV. The critical temperature is $T_{cr} = 0.57$ MeV.

Fig. 12. Specific heat as a function of temperature obtained using the most probable Δ (thin line) and using the average Δ (thick line).

Fig. 13. Entropy as a function of temperature and angular momentum for the uniform model. The lowest isotherm is at $T = 0.158\ T_{cr}$ and the spacing between the isotherms is $0.053\ T_{cr}$.

Fig. 14. Entropy as a function of temperature and angular momentum for the proton a) and neutron b) components of $^{194}_{78}Pt$.

Fig. 15. Yrast line and higher isotherms for the uniform model. The isotherm next to the yrast line is at $T = 0.158\ T_{cr}$ and the spacing between isotherms is $0.0526\ T_{cr}$. The dashed line represents the yrast line of the unpaired system and the upper line crossing the isotherms is the boundary of the superfluid phase. For the energy unit see caption to fig. 9.

Fig. 16. Yrast lines and higher isotherms for the proton a) and neutron b) components of $^{194}_{78}Pt$.

Fig. 17. Square root of the denominator determinant (in MeV) for the nucleus $^{194}_{78}Pt$ as a whole, as a function of temperature and angular momentum. The two discontinuities associated with the proton and neutron phase transitions are observed in many isotherms.

Fig. 18. Lines of constant entropy in the temperature-angular momentum plane for the nuclei $^{194}_{78}Pt$ a); $^{198}_{80}Hg$ b); $^{220}_{86}Rn$ c). The boundaries of the proton and neutron superfluid phases are also shown.

Fig. 19. Lines of constant entropy in the energy angular momentum plane for the same nuclei as in fig. 18. The yrast line and the boundaries of the neutron and proton superfluid phases are also shown.

Fig. 20. Lines of constant natural logarithm of the level density in the energy angular momentum plane for the same nuclei as in fig. 18. The yrast line and the boundaries of the neutron and proton superfluid phases are also shown.

0 0 0 0 3 8 0 0 1 8 7

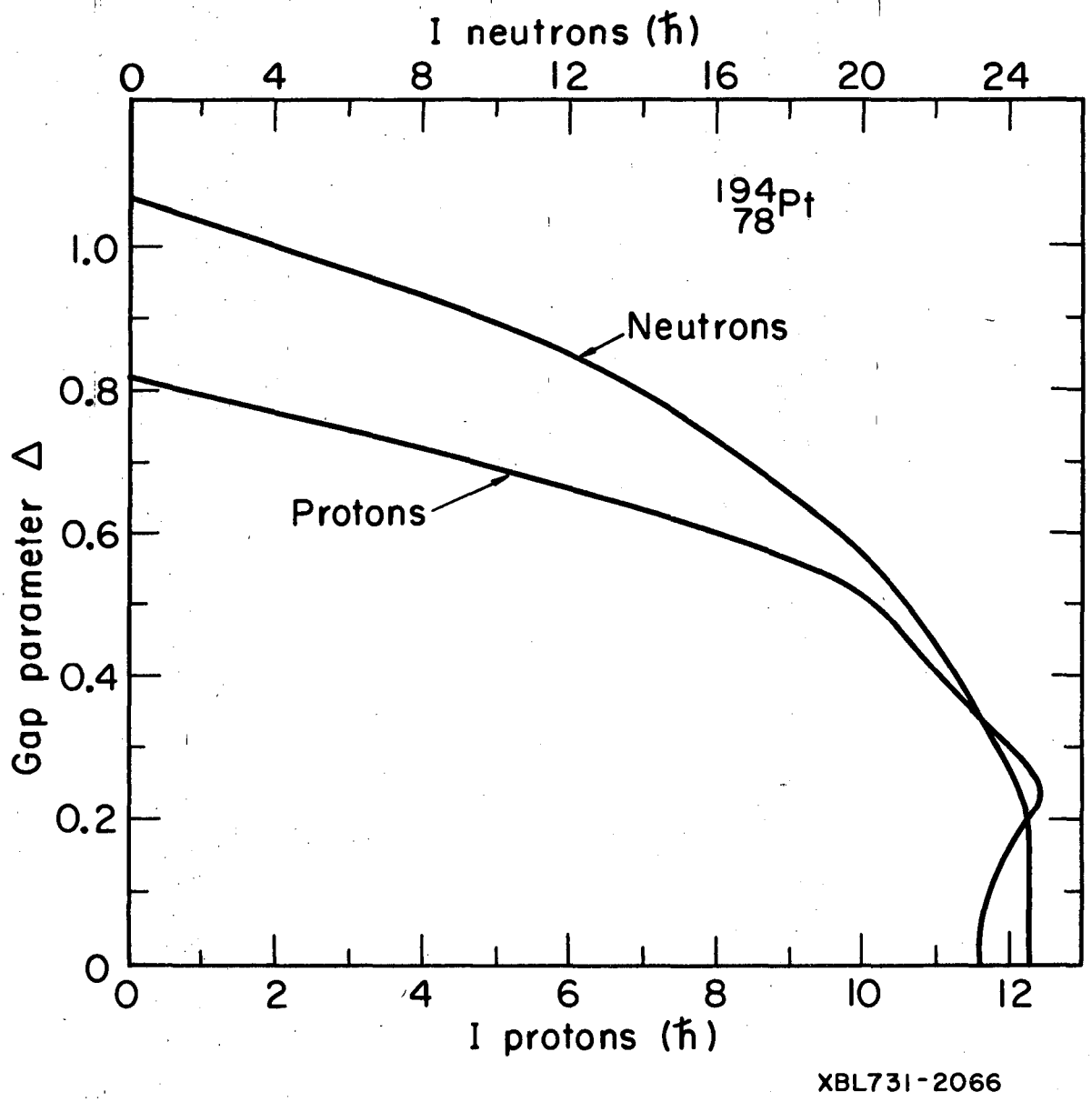

Fig. 1

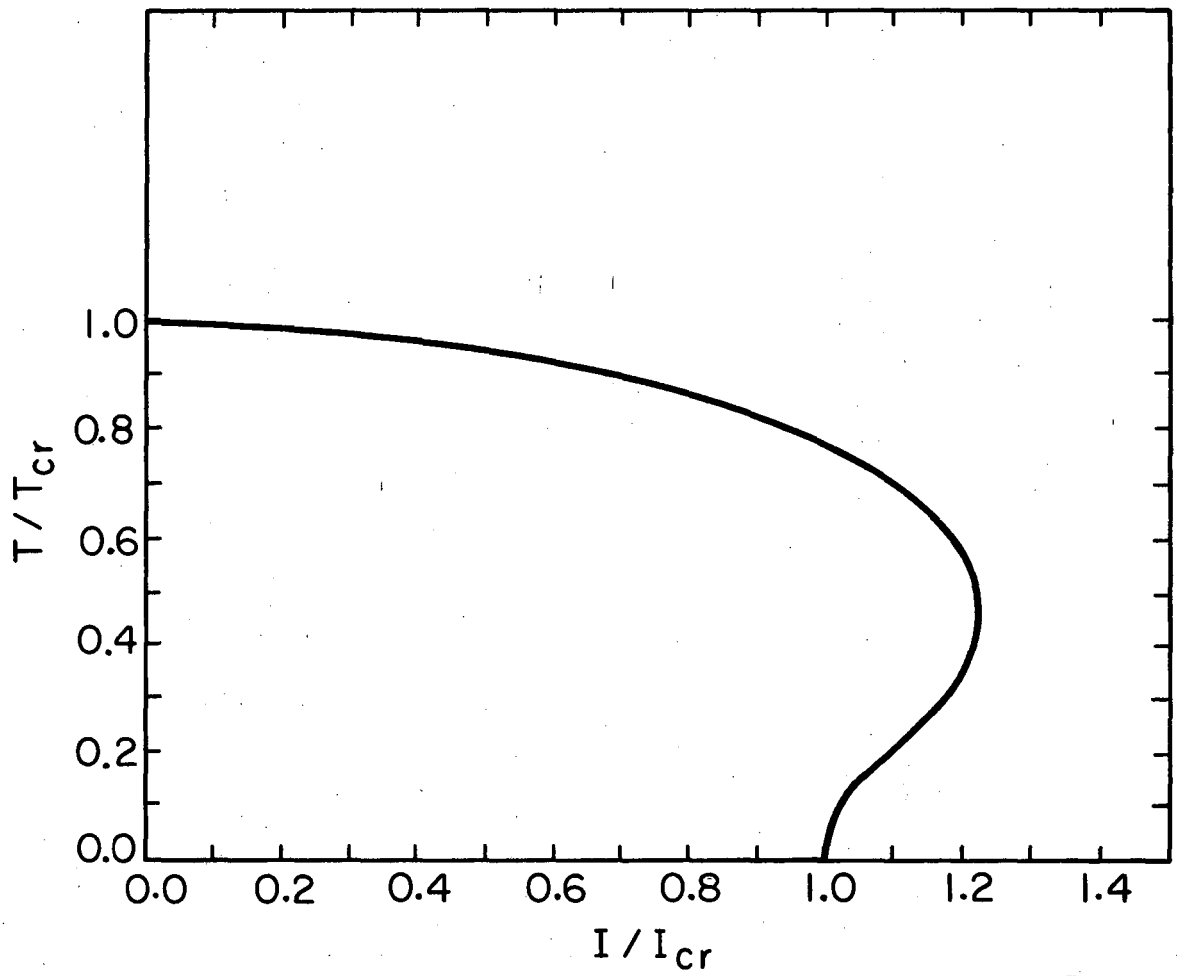

XBL 734-421

Fig. 2

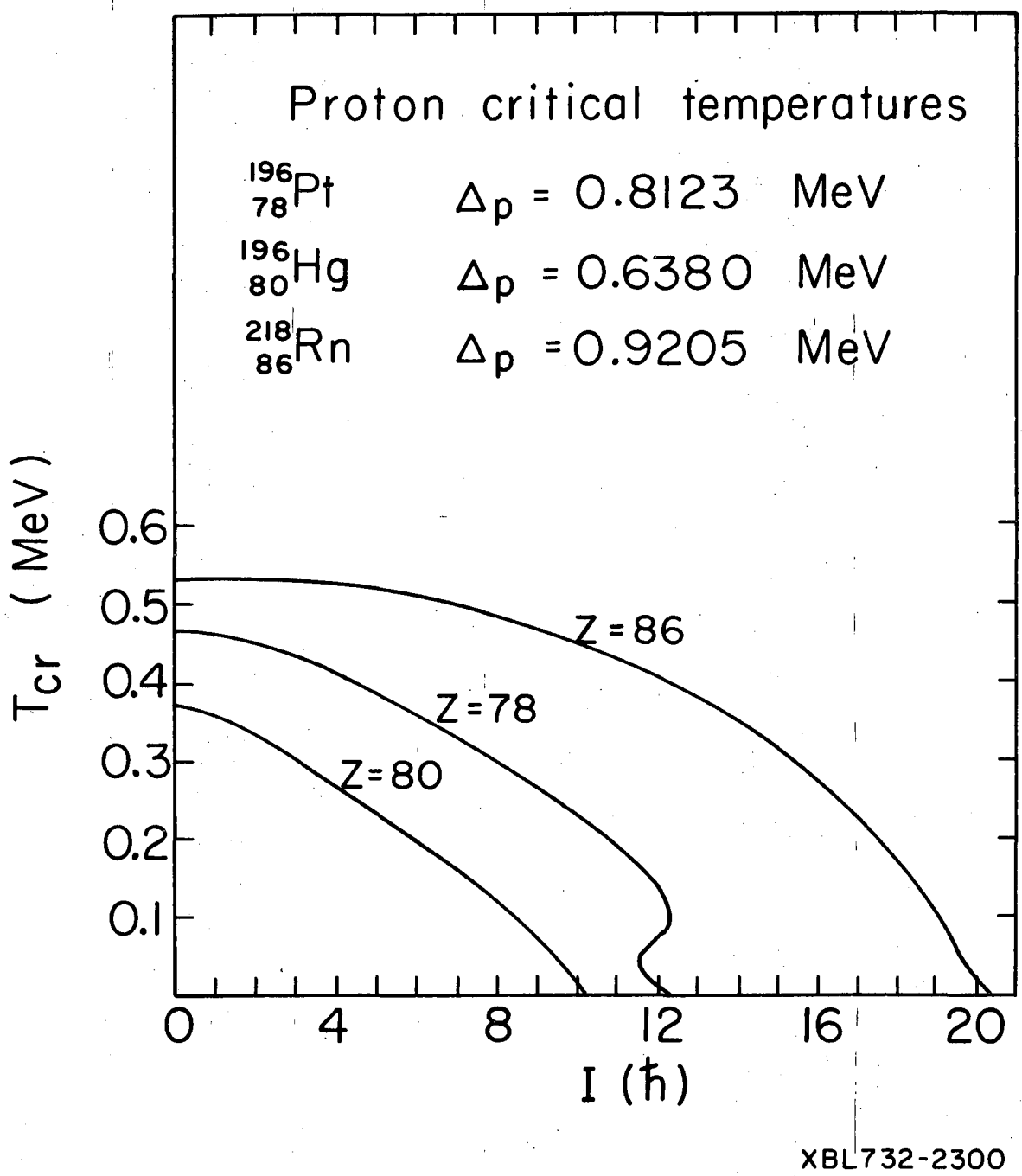
Proton critical temperatures
$^{196}_{78}$Pt Δ_p = 0.8123 MeV
$^{196}_{80}$Hg Δ_p = 0.6380 MeV
$^{218}_{86}$Rn Δ_p = 0.9205 MeV
T_{cr} (MeV)
0.6
0.5
0.4
0.3
0.2
0.1
Z=86
Z=78
Z=80
0
4
8
12
16
20
I (ħ)
XBL732-2300

Fig. 3a

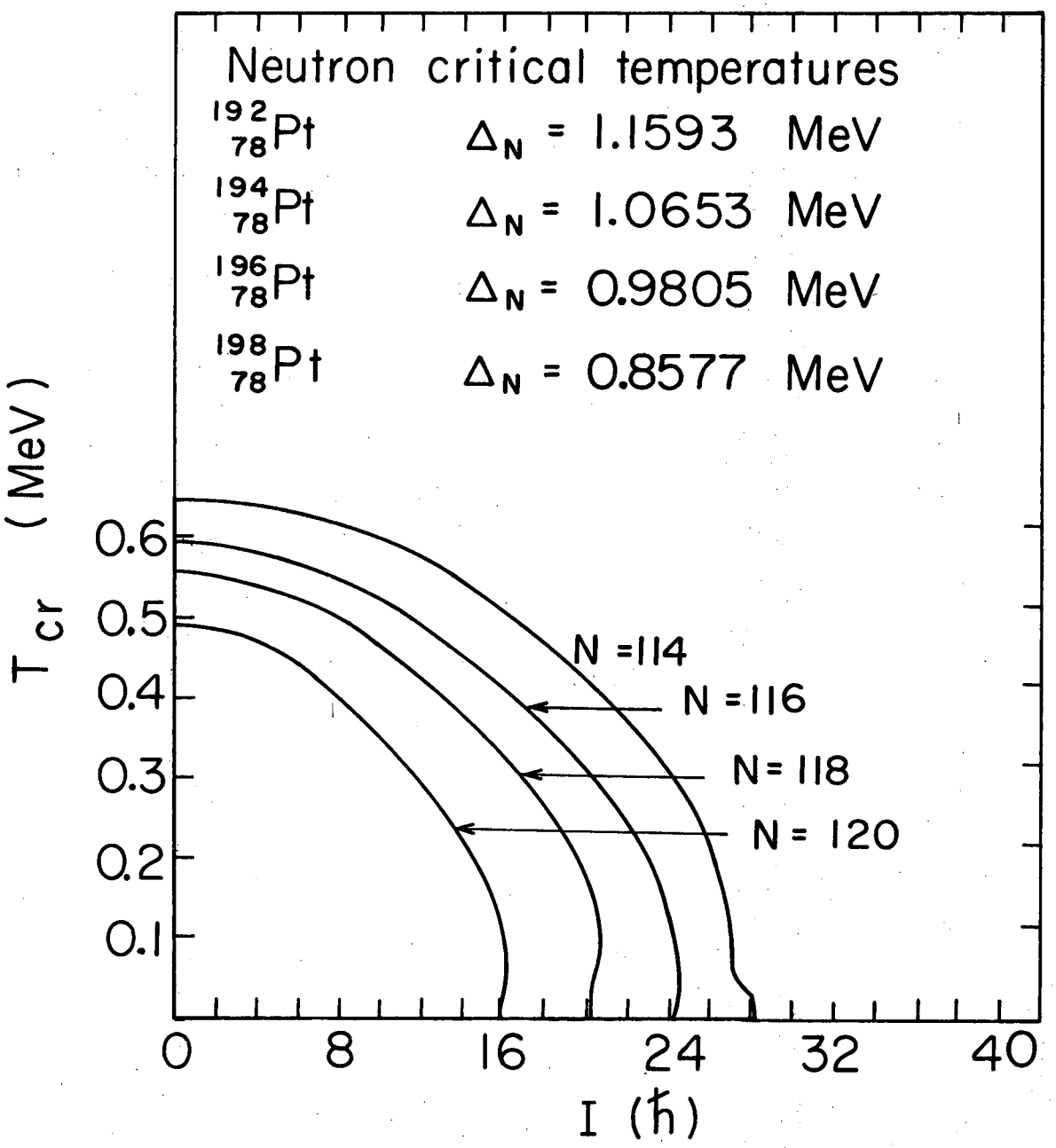

XBL732-2299

Fig. 3b

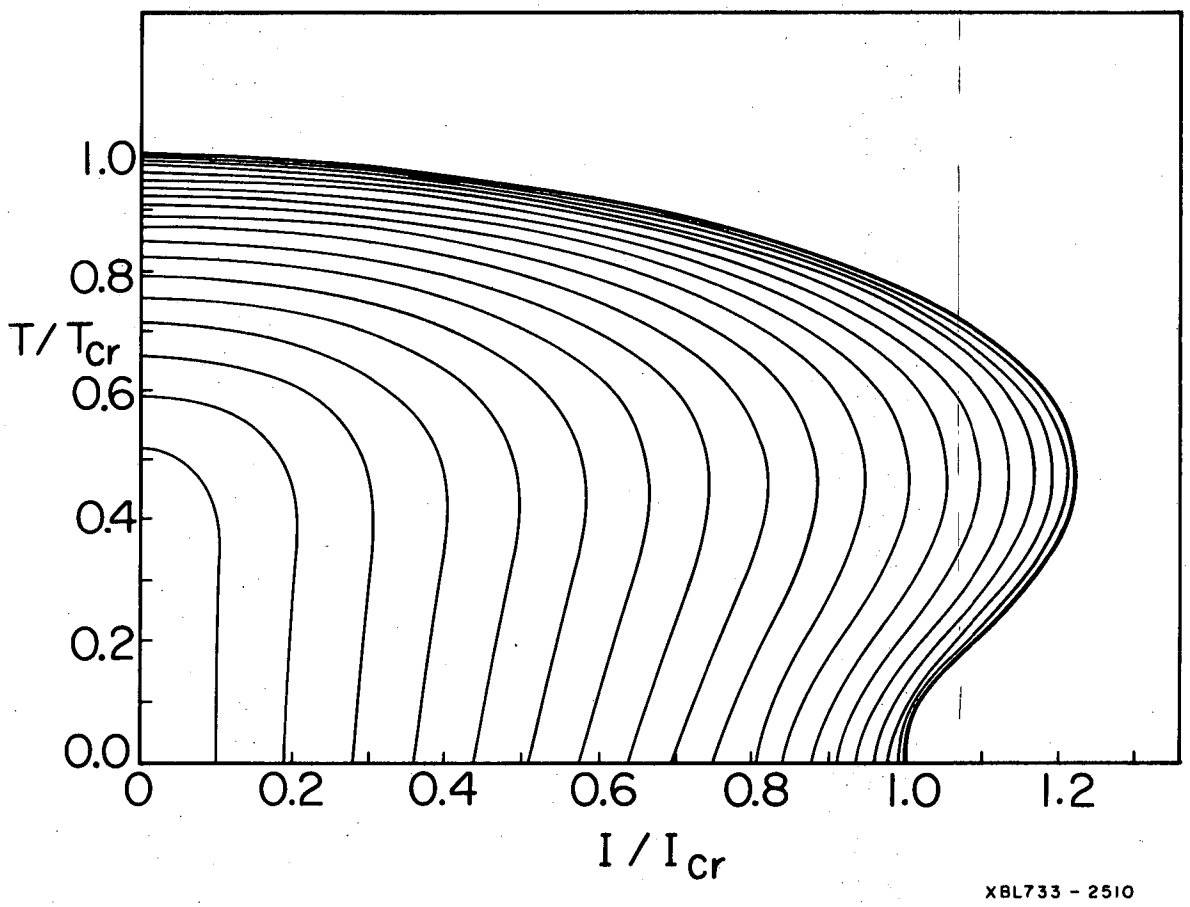

Fig. 4

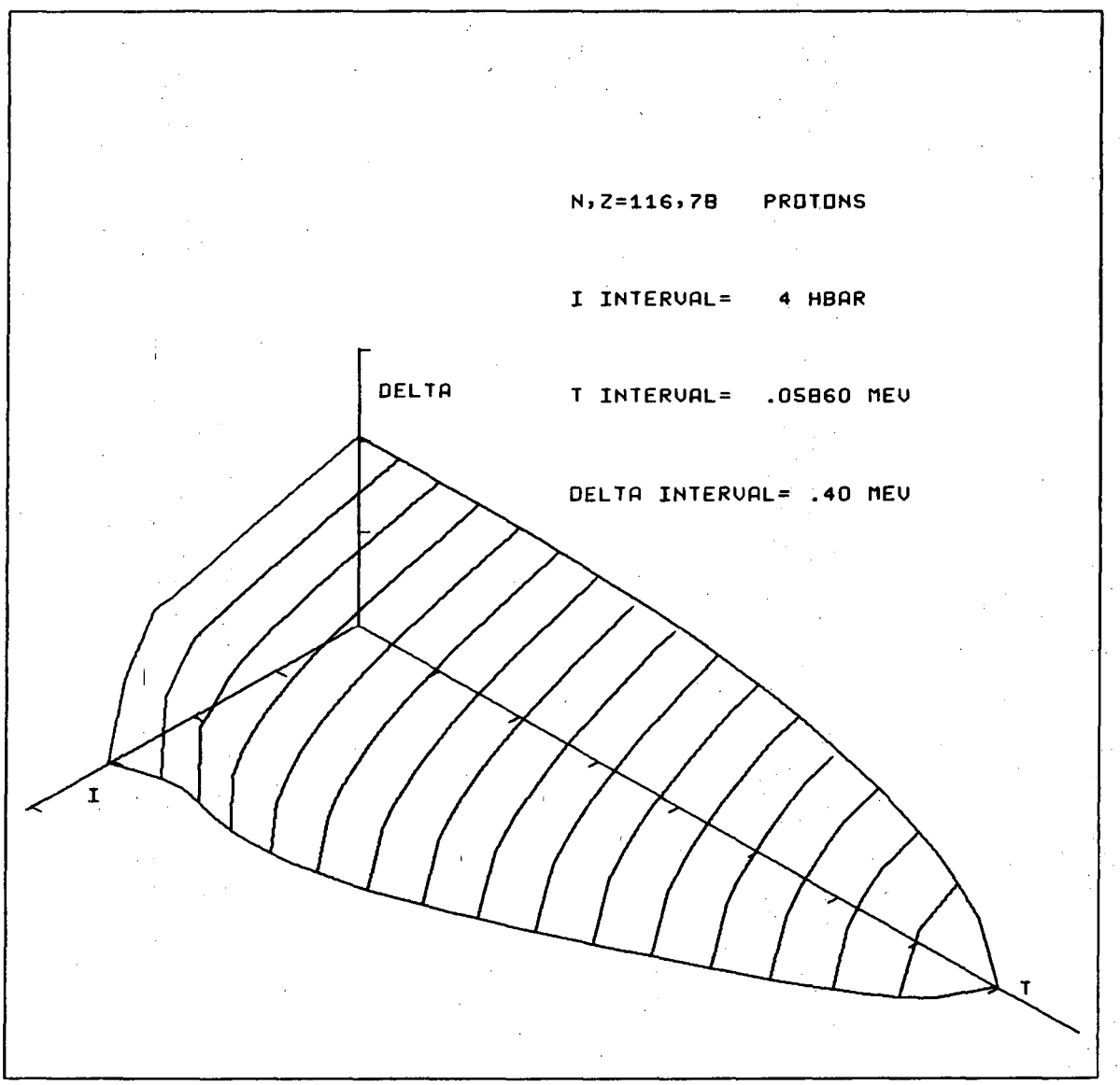

XBL 731-30

Fig. 5a

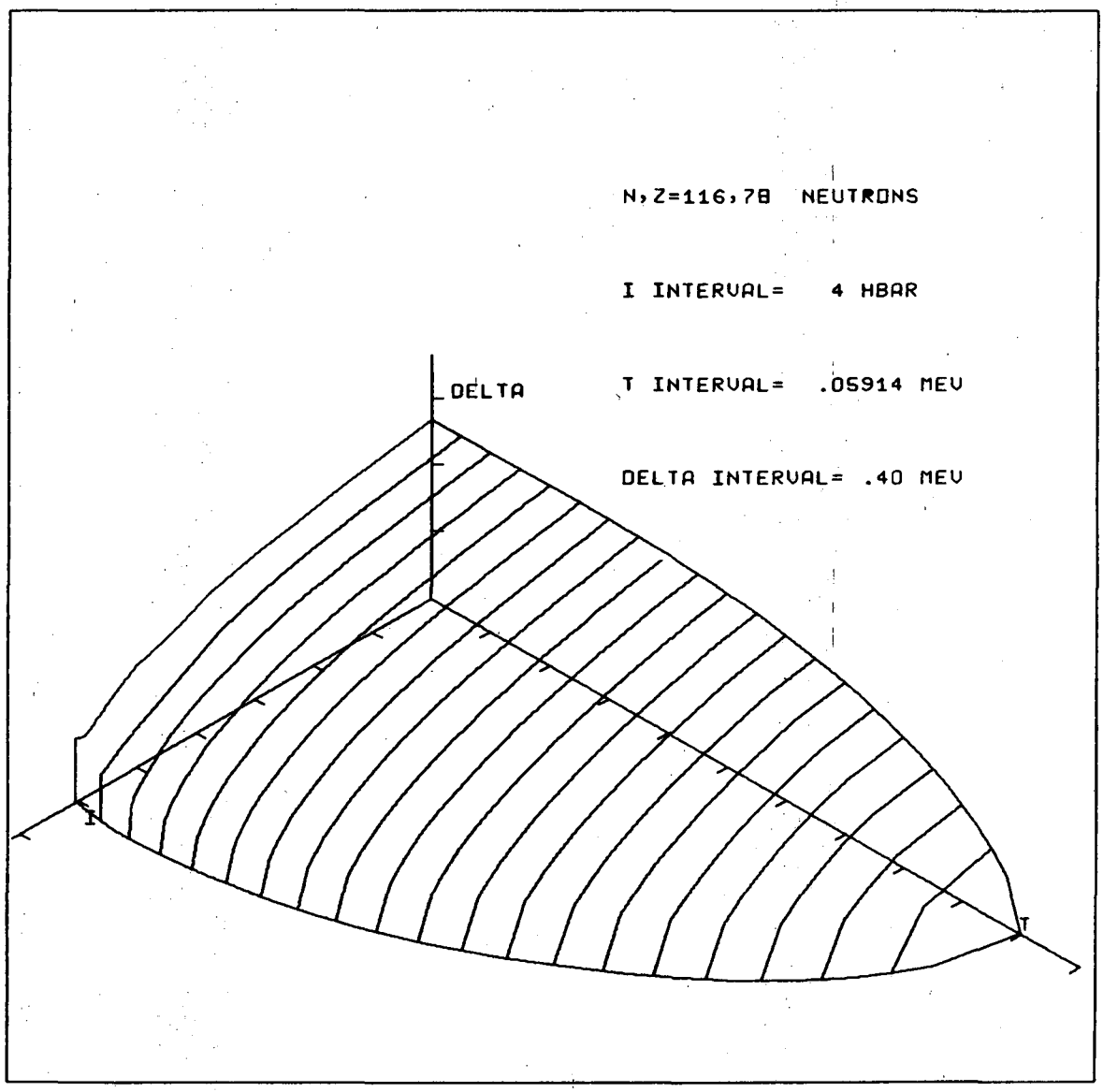

XBL 731-31

Fig. 5b

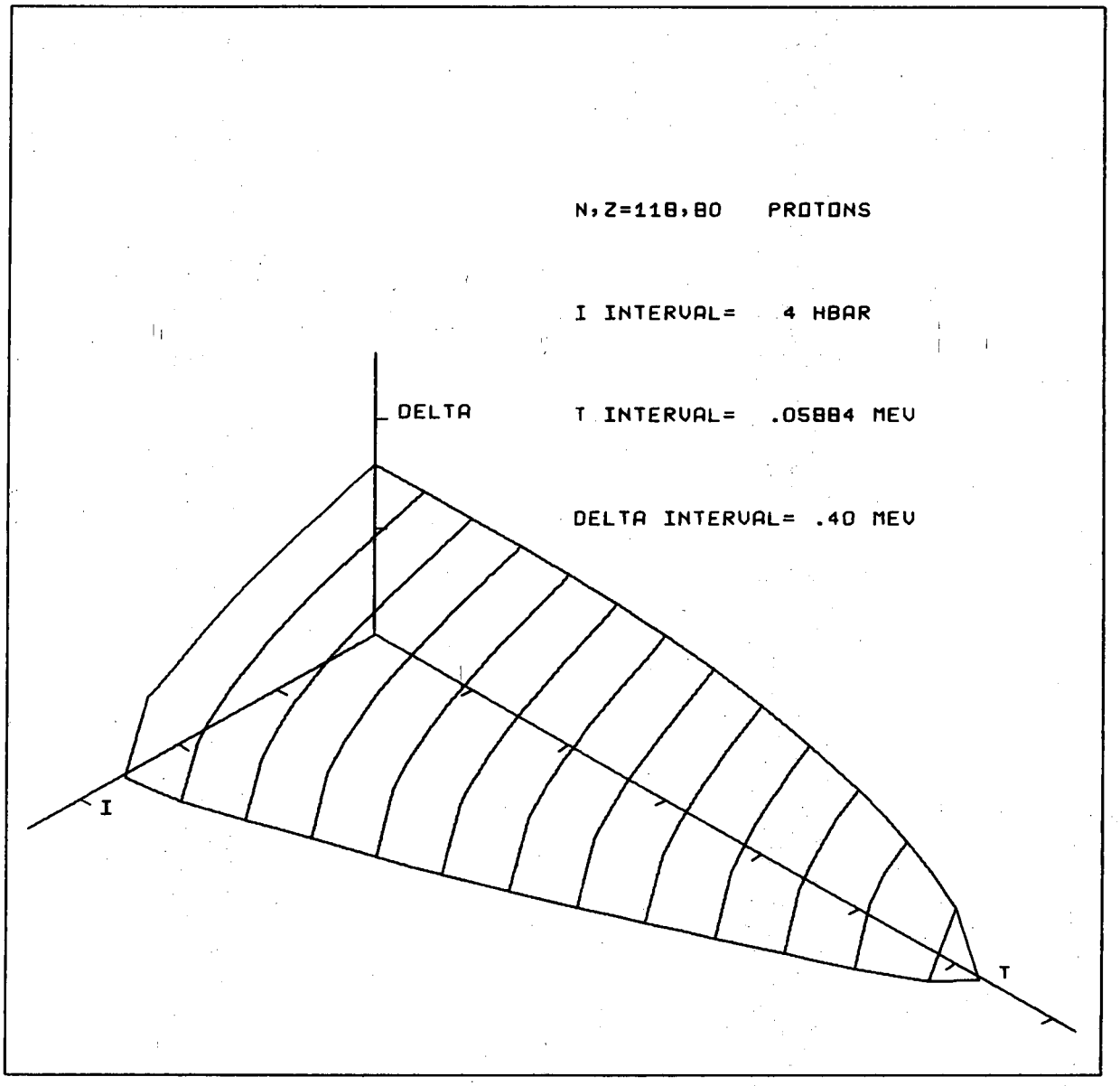

XBL 733-272

Fig. 5c

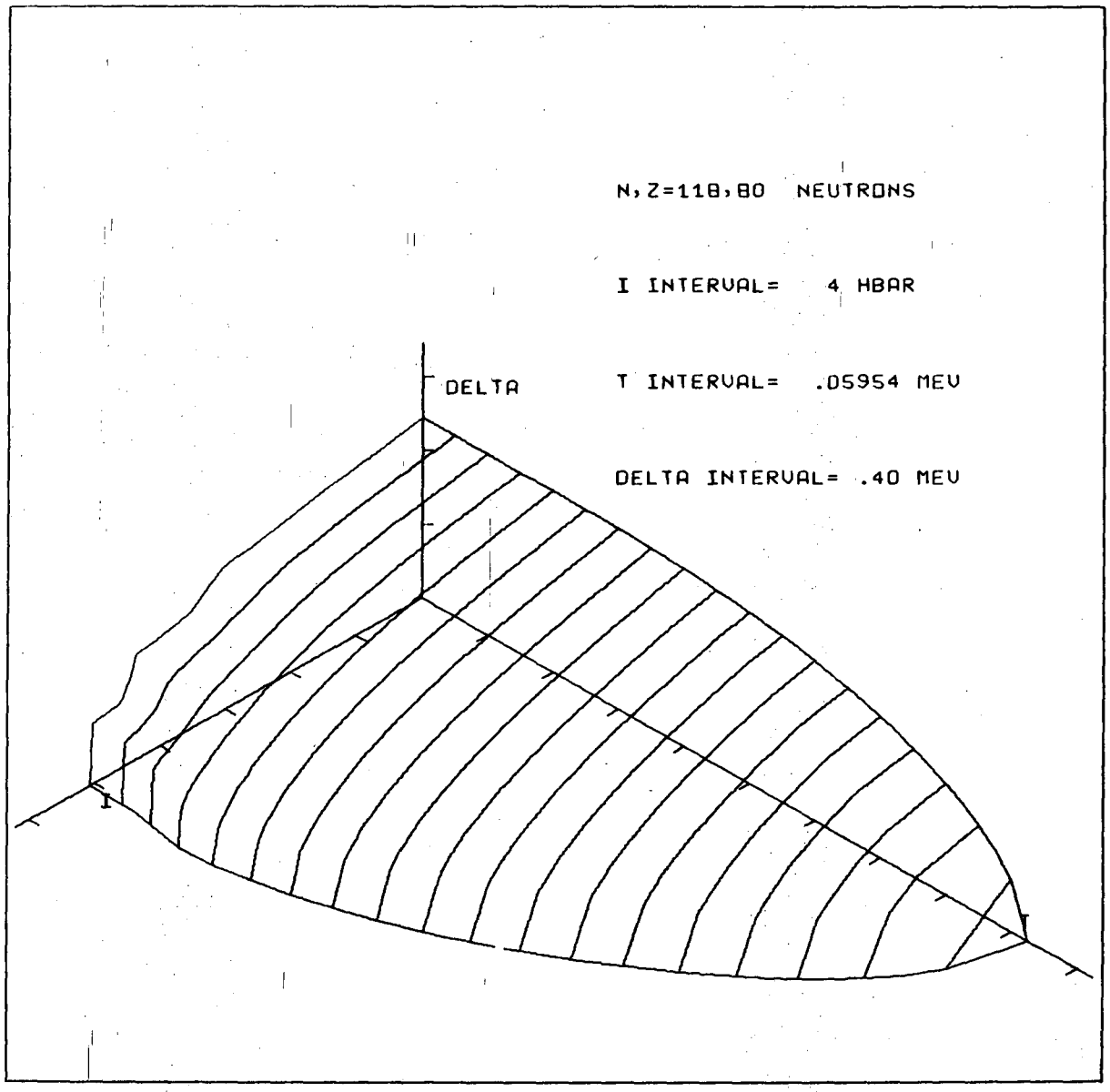

XBL 733-271

Fig. 5d

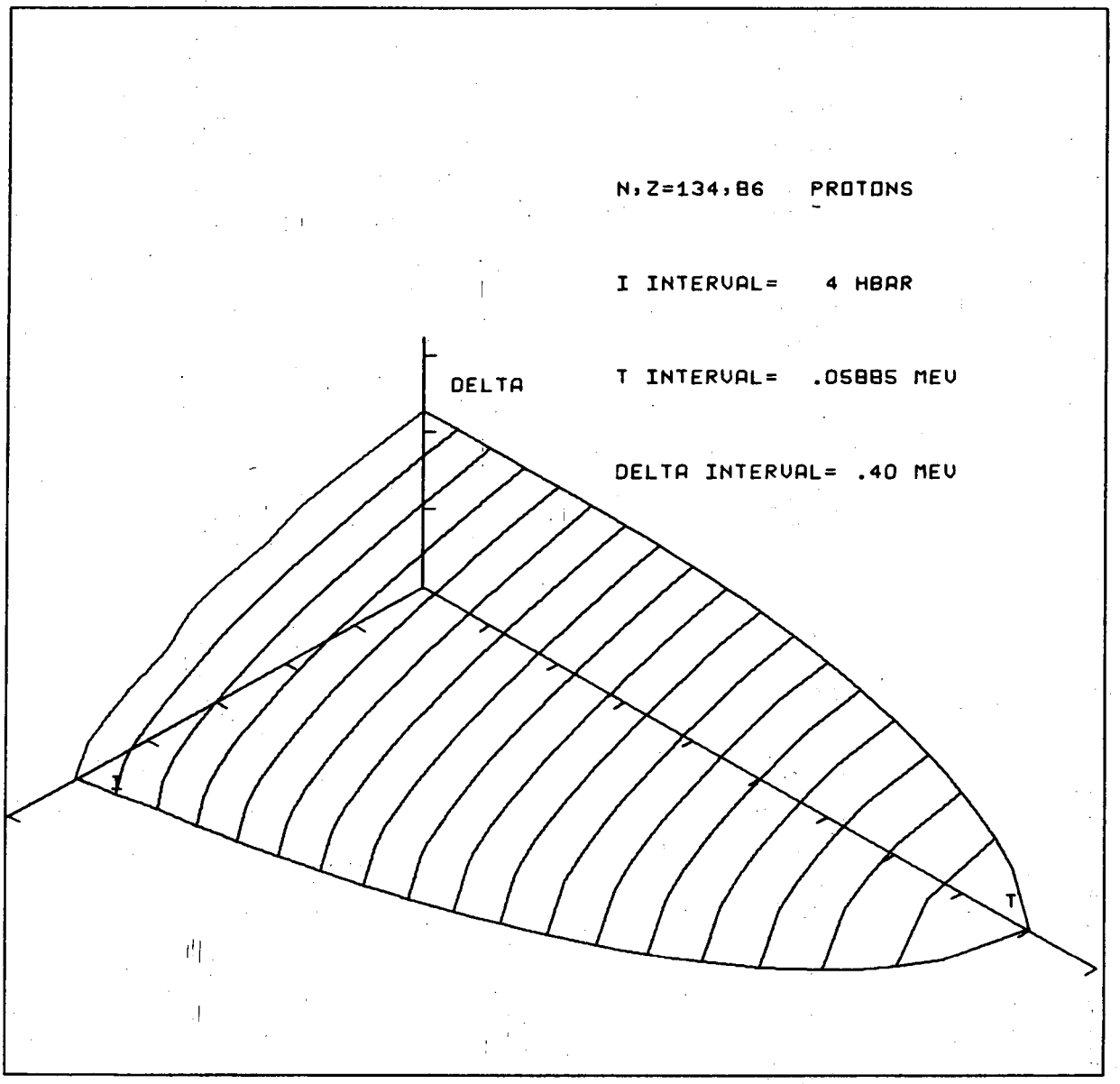

XBL 733-270

Fig. 5e

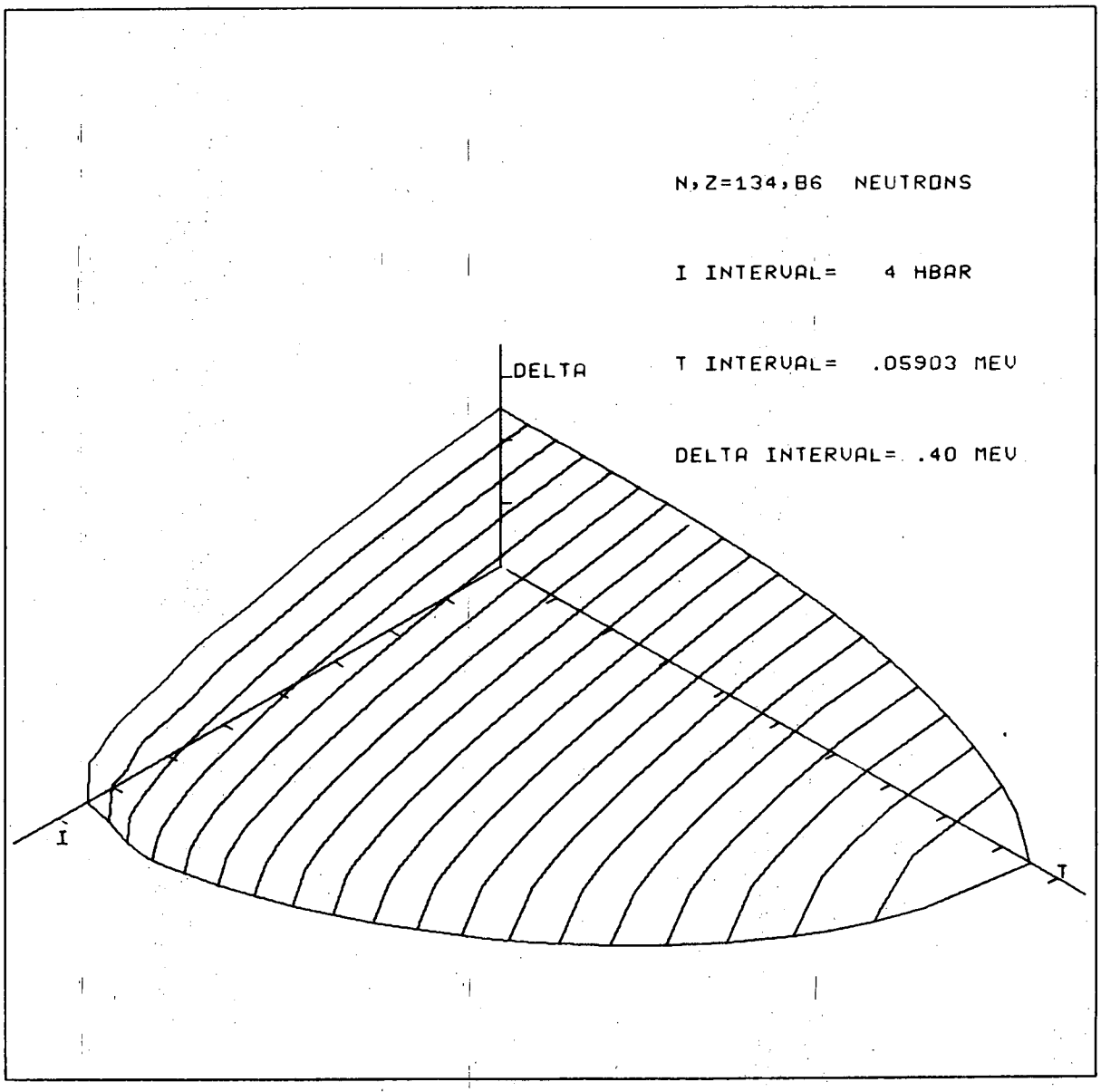

XBL 733-273

Fig. 5f

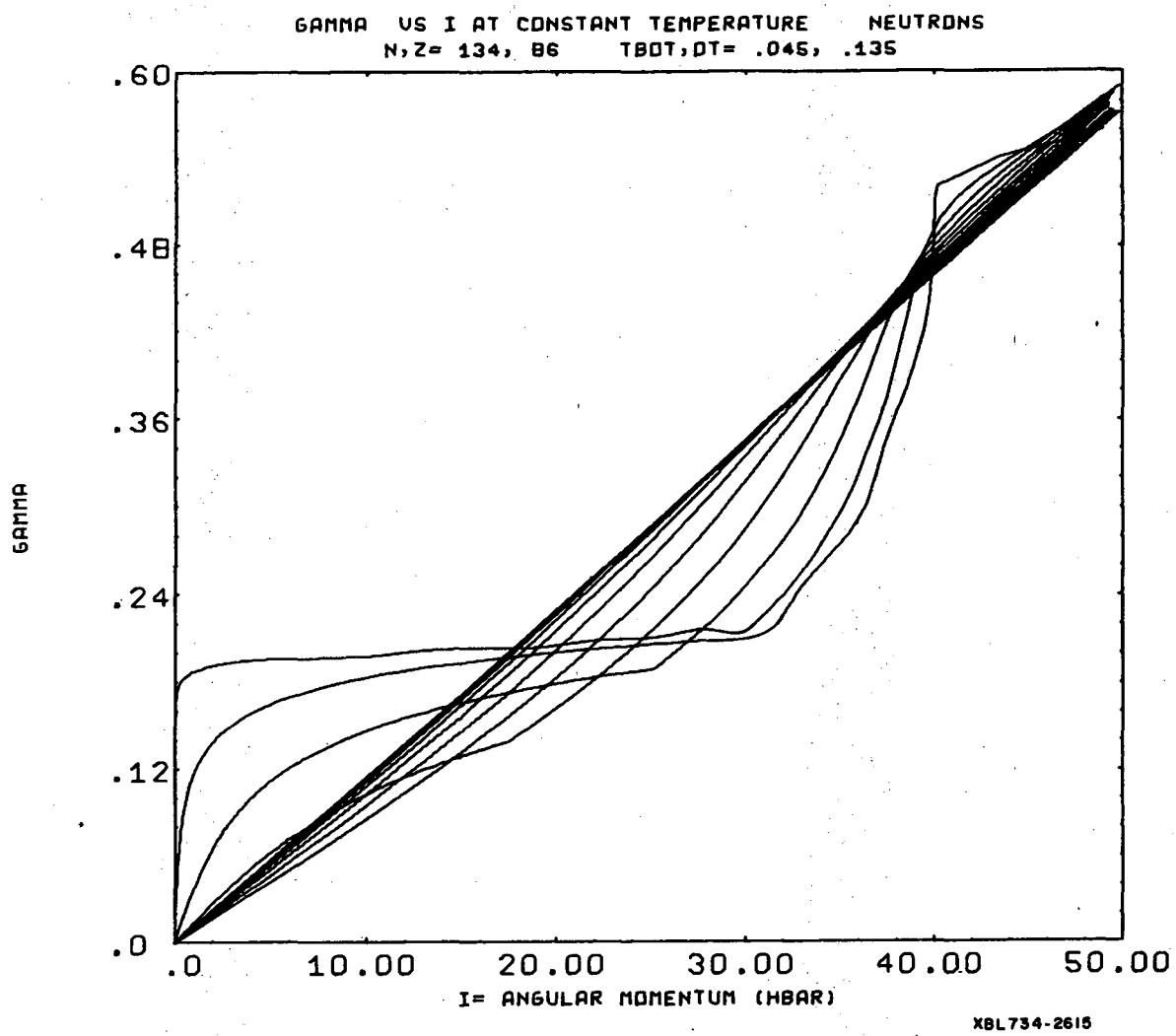
GAMMA VS I AT CONSTANT TEMPERATURE NEUTRONS
N,Z= 134, 86 TBOT,DT= .045, .135
.60
.48
.36
.24
.12
.0
GAMMA
.0
10.00
20.00
30.00
40.00
50.00
I= ANGULAR MOMENTUM (HBAR)
XBL734-2615

Fig. 6

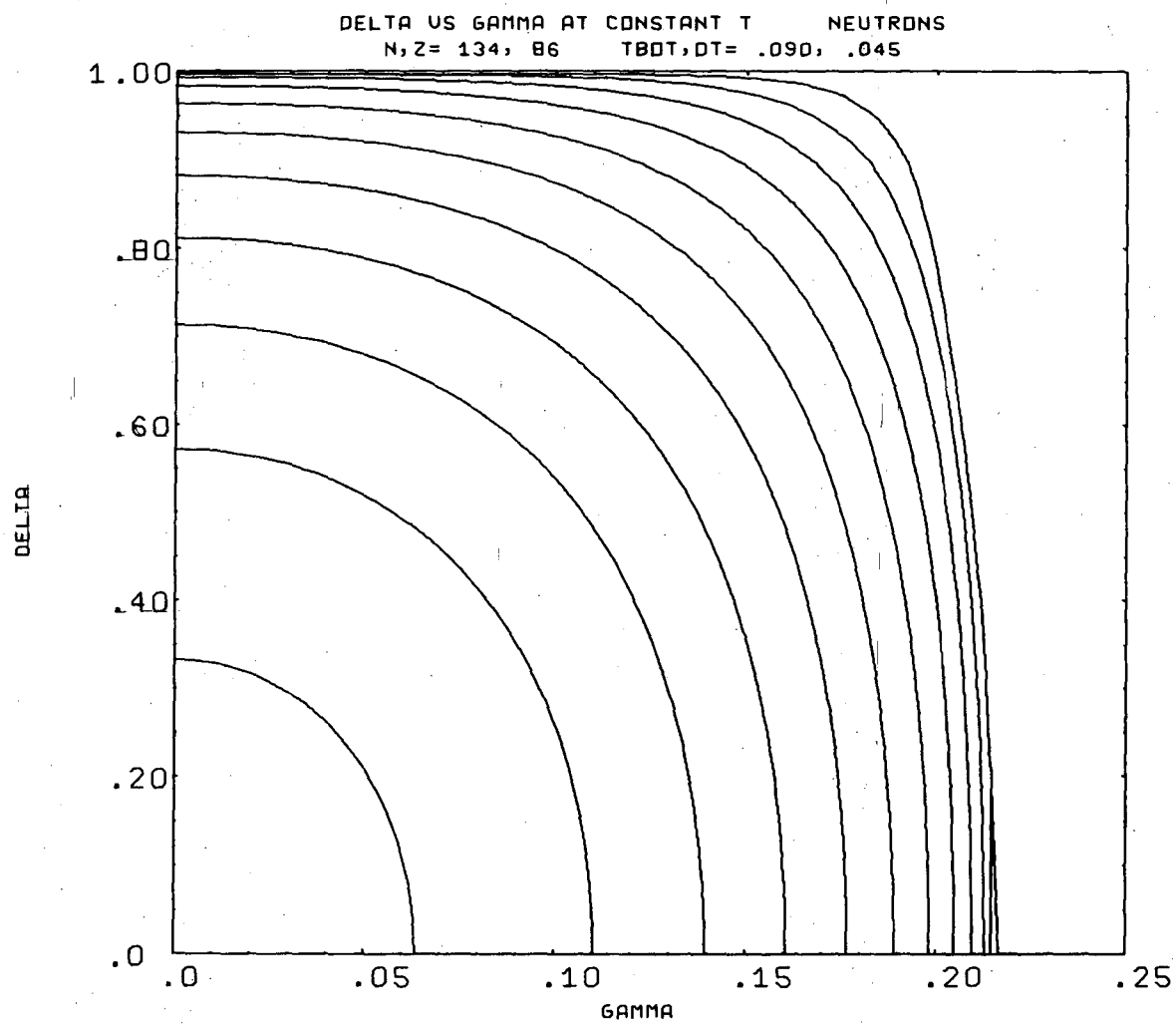

XBL 734-419

Fig. 7

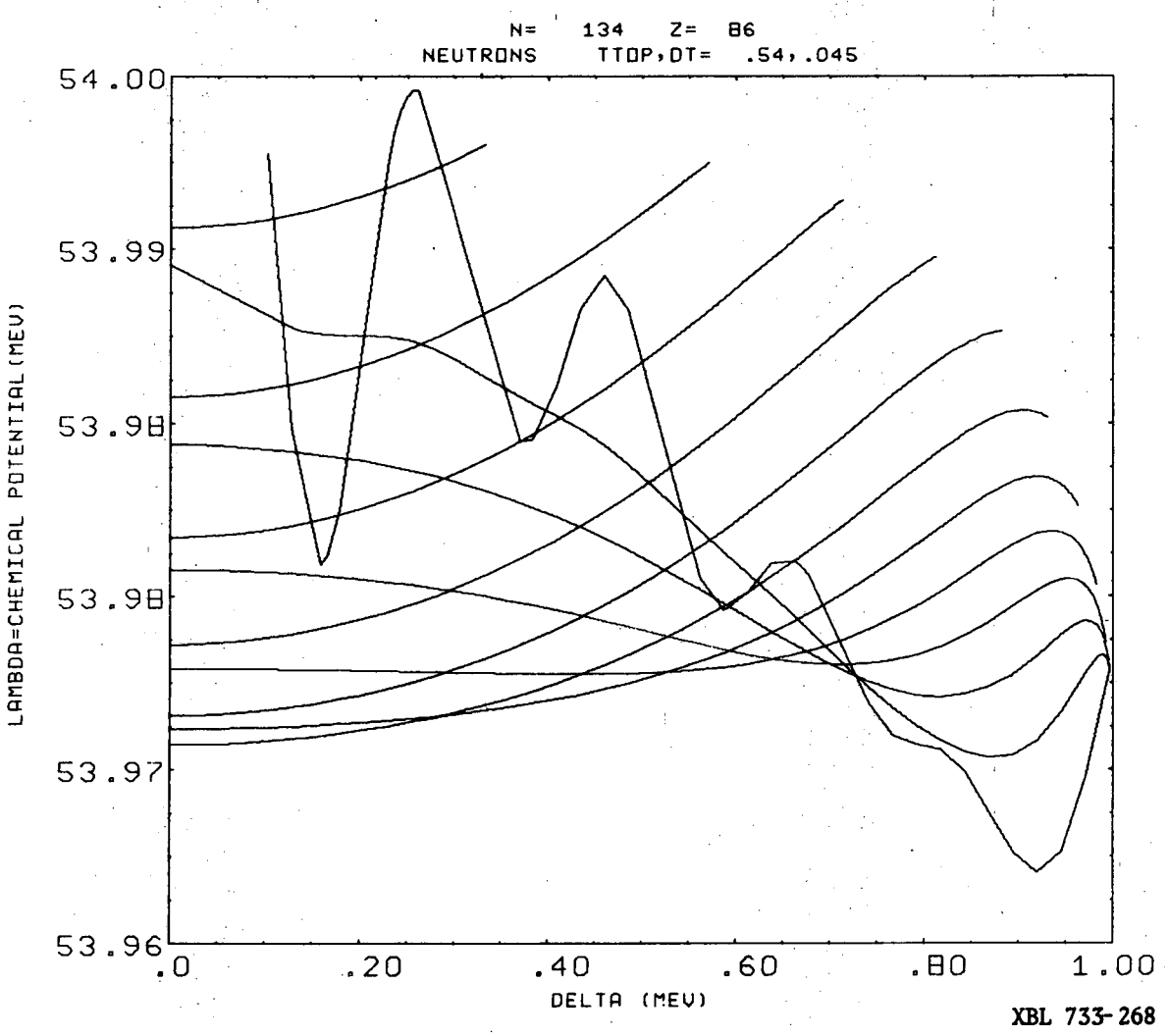
N= 134 Z= 86
NEUTRONS TTOP,DT= .54,.045
54.00
53.99
53.98
53.98
53.97
53.96
LAMBDA=CHEMICAL POTENTIAL(MEV)
.0
.20
.40
.60
.80
1.00
DELTA (MEV)
XBL 733-268

Fig. 8

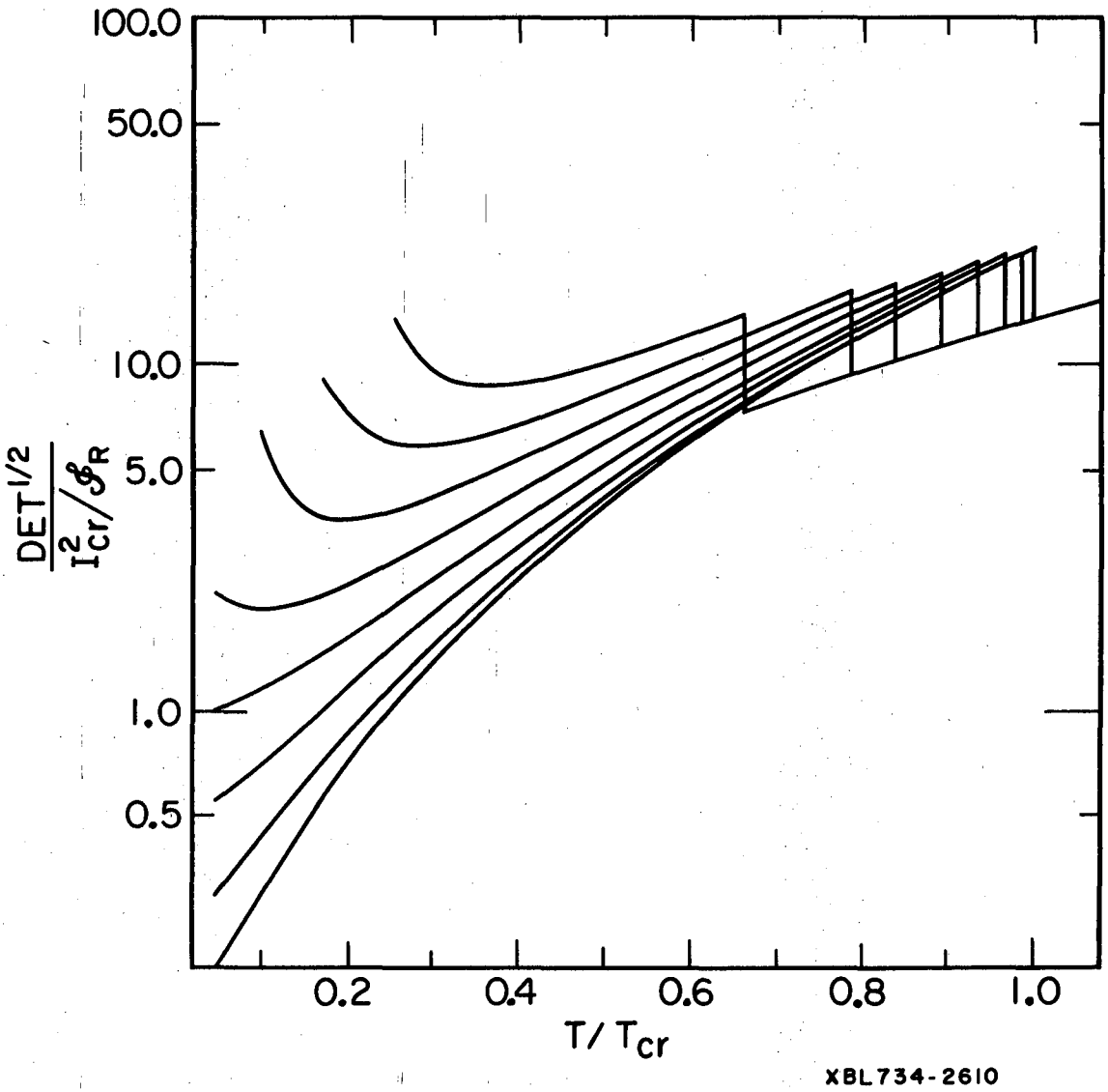
100.0
50.0
10.0
5.0
1.0
0.5
$\frac{DET^{1/2}}{I_{cr}^2/\mathcal{S}_R}$
0.2
0.4
0.6
0.8
1.0
T/T_{cr}
XBL734-2610

Fig. 9

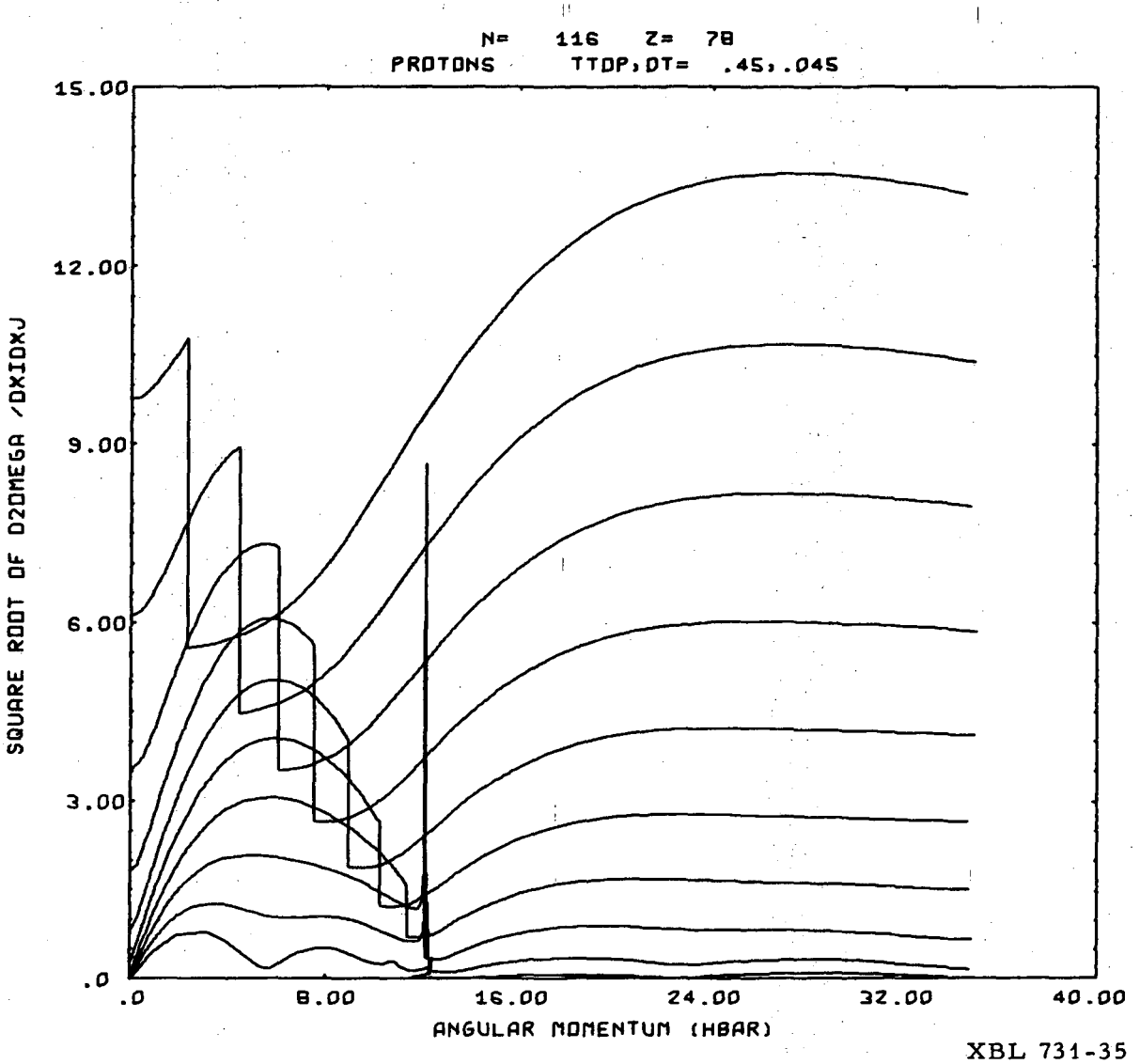

XBL 731-35

Fig. 10a

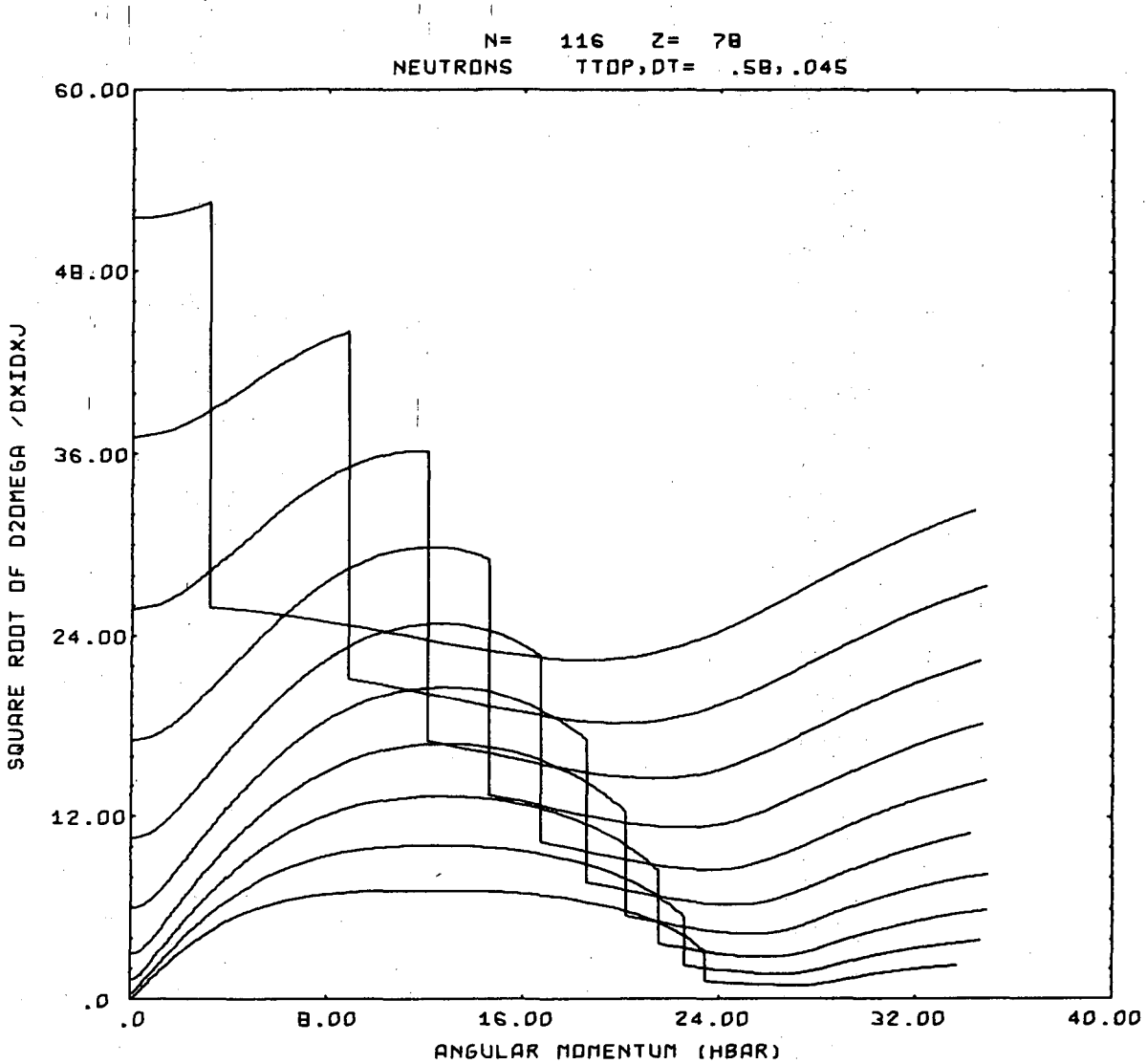

XBL 731-34

Fig. 10b

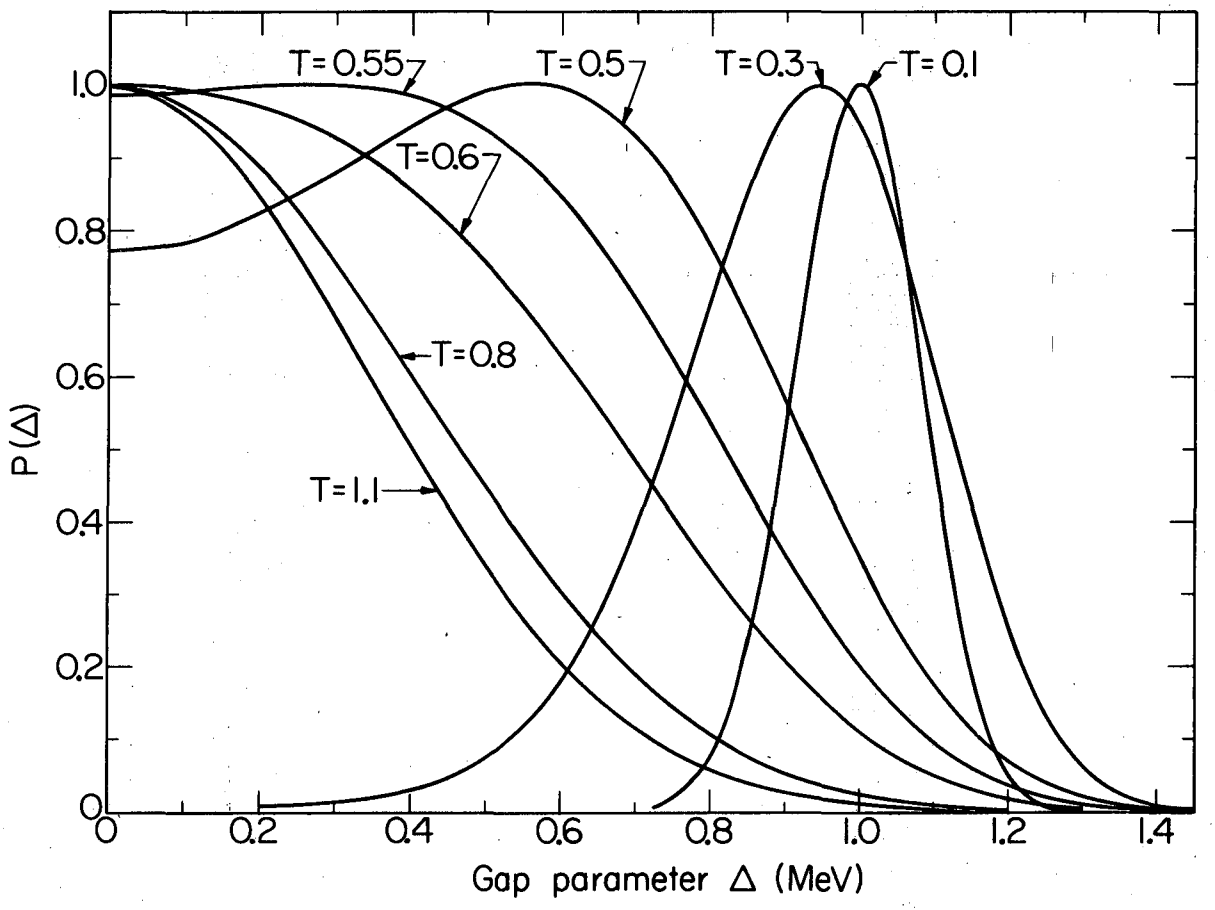

XBL724-2698

Fig. 11

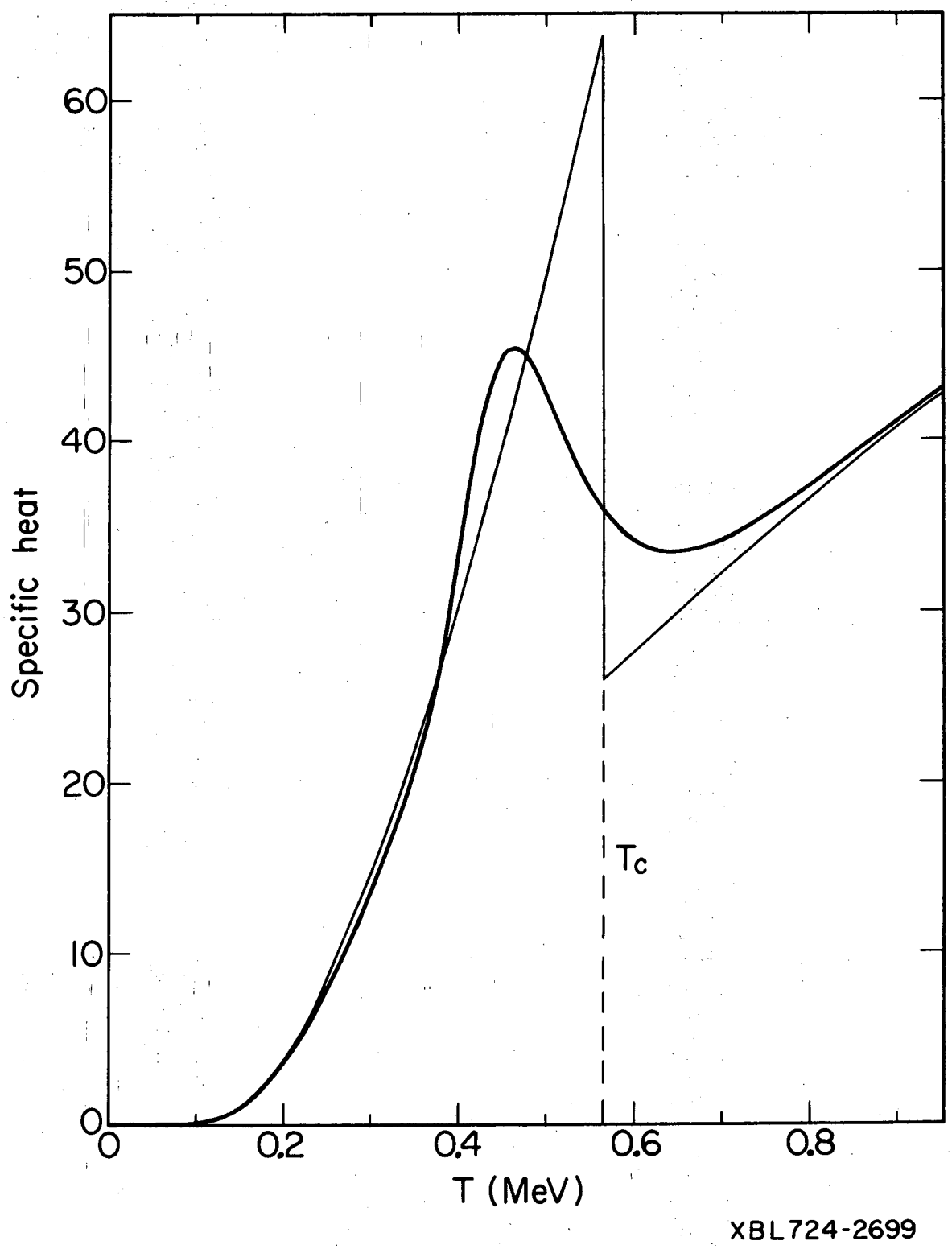
60
50
40
30
20
10
0
Specific heat
0
0.2
0.4
0.6
0.8
T (MeV)
Tc
XBL724-2699

Fig. 12

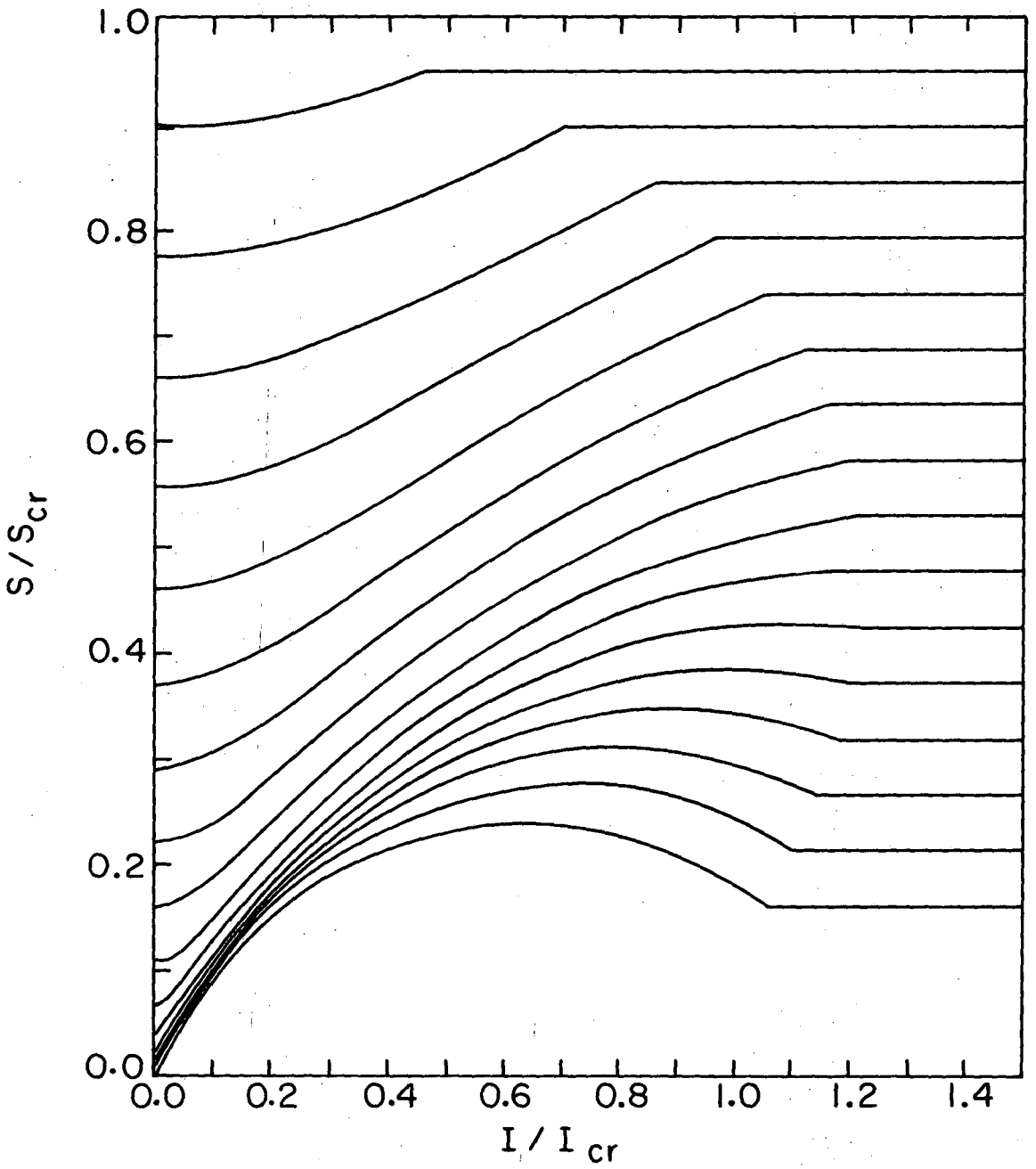

XBL 734-422

Fig. 13

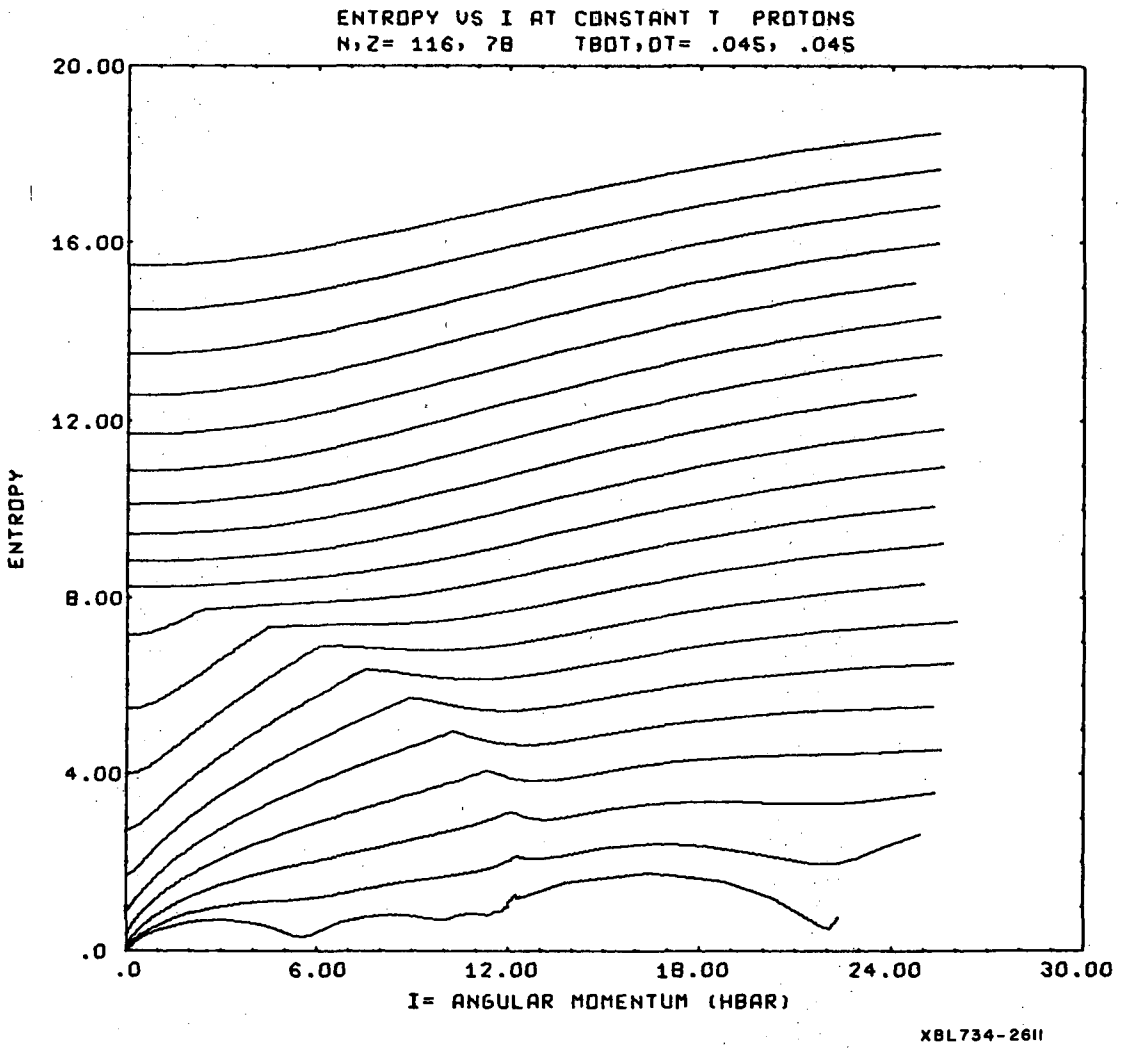
ENTROPY VS I AT CONSTANT T PROTONS
N,Z= 116, 78 TBOT,DT= .045, .045
20.00
16.00
12.00
8.00
4.00
.0
ENTROPY
.0
6.00
12.00
18.00
24.00
30.00
I= ANGULAR MOMENTUM (HBAR)
XBL734-2611

Fig. 14a

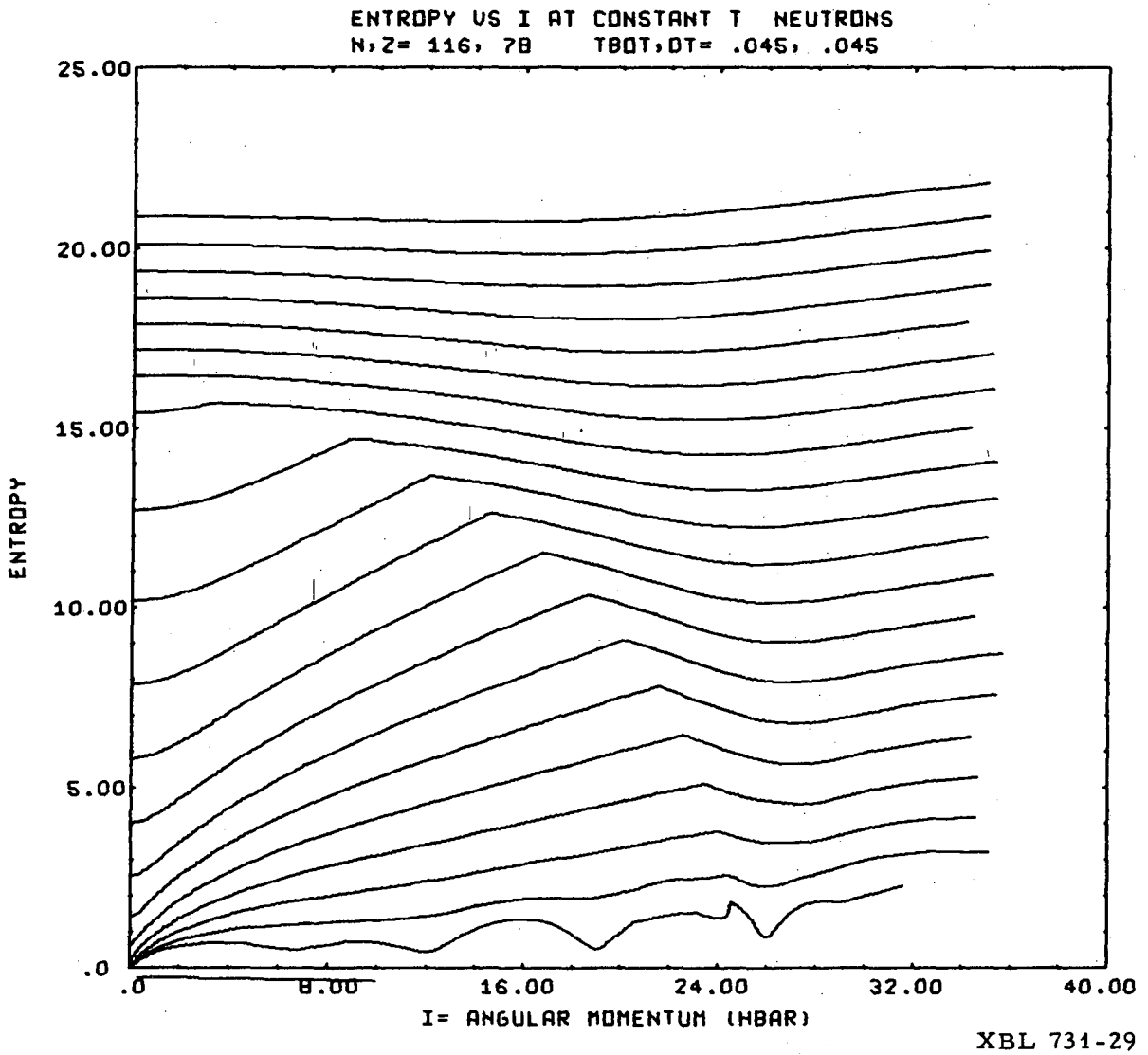

XBL 731-29

Fig. 14b

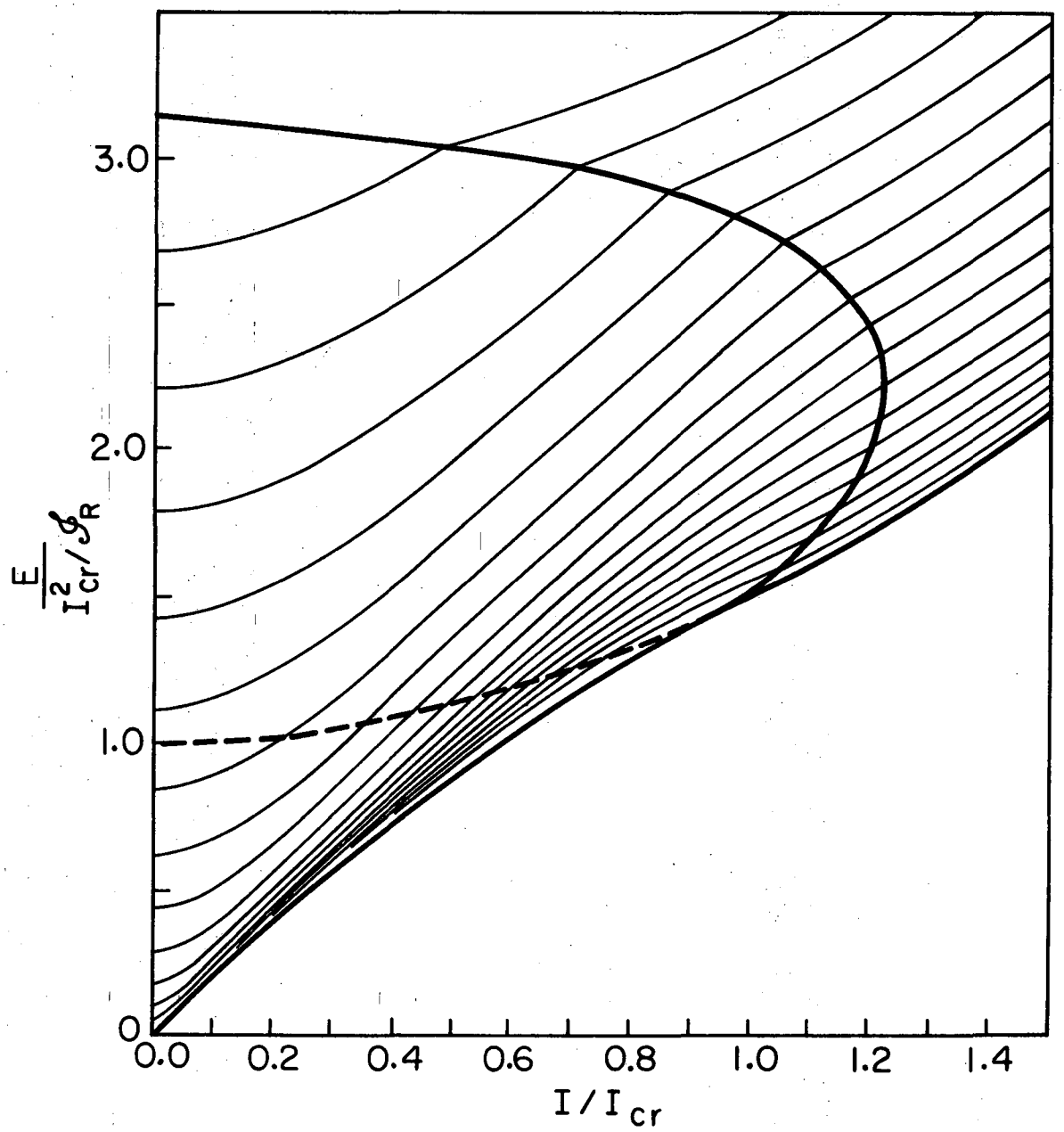

XBL733-2511

Fig. 15

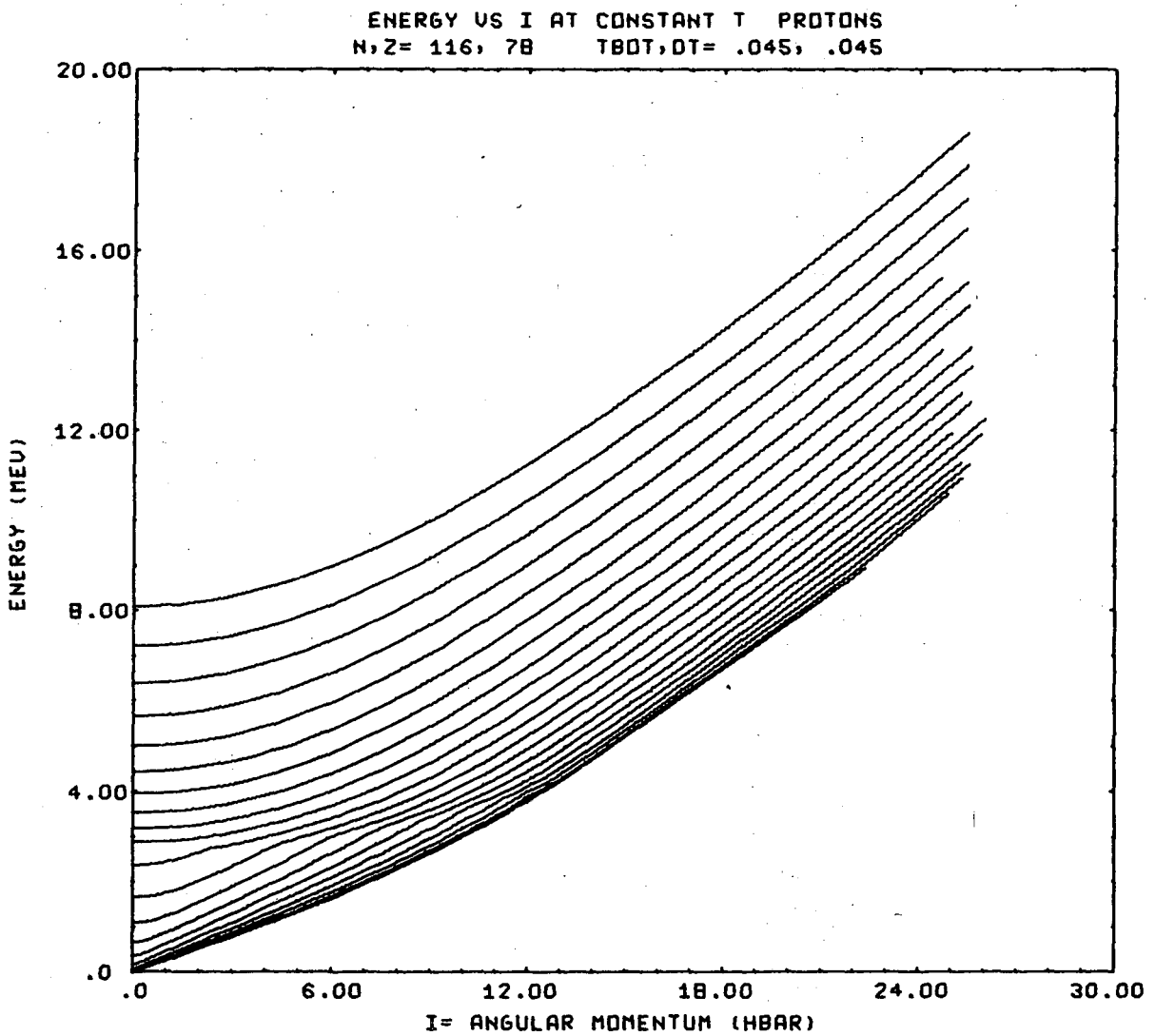

XBL 731-26

Fig. 16a

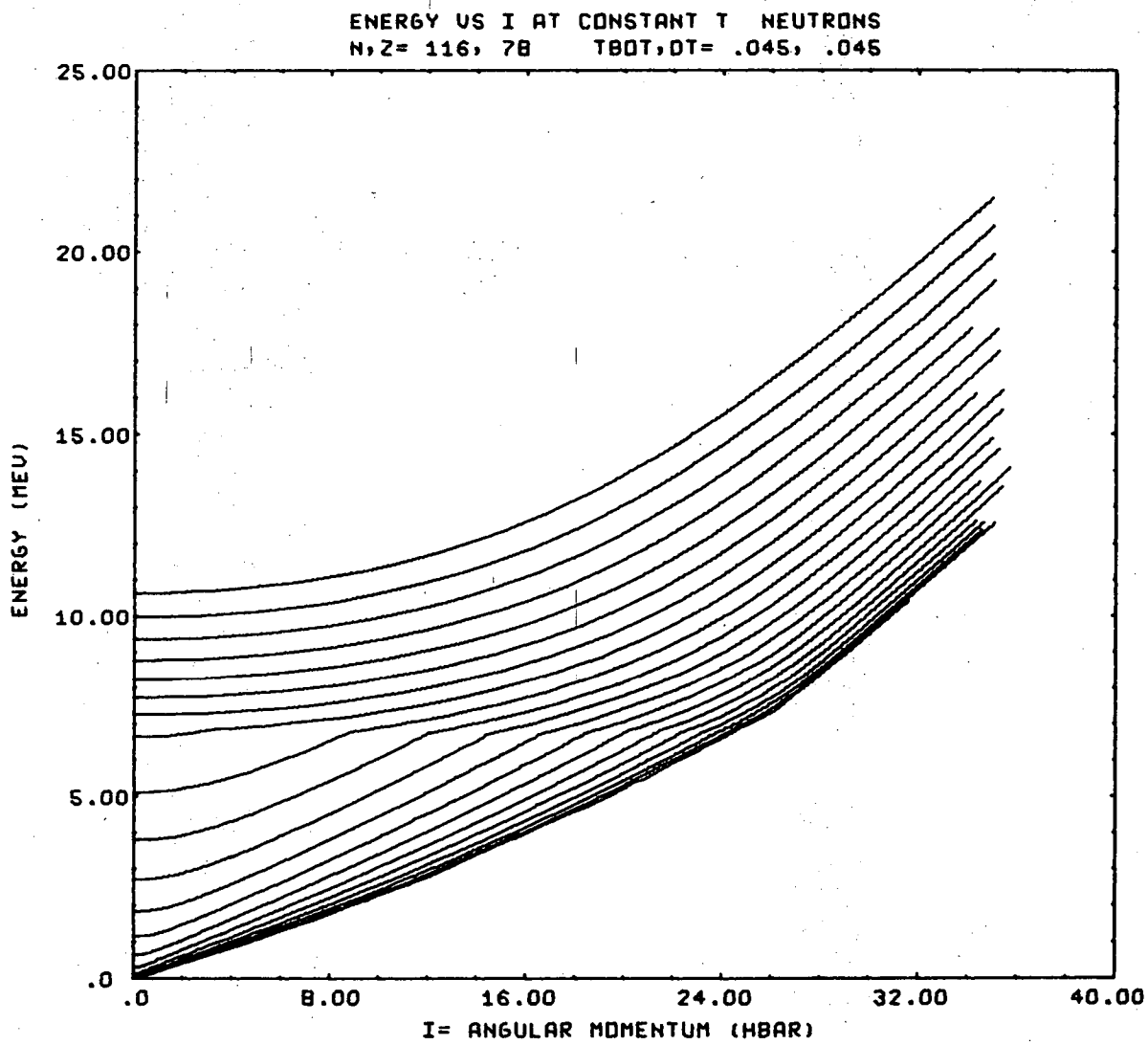

XBL 731-27

Fig. 16b

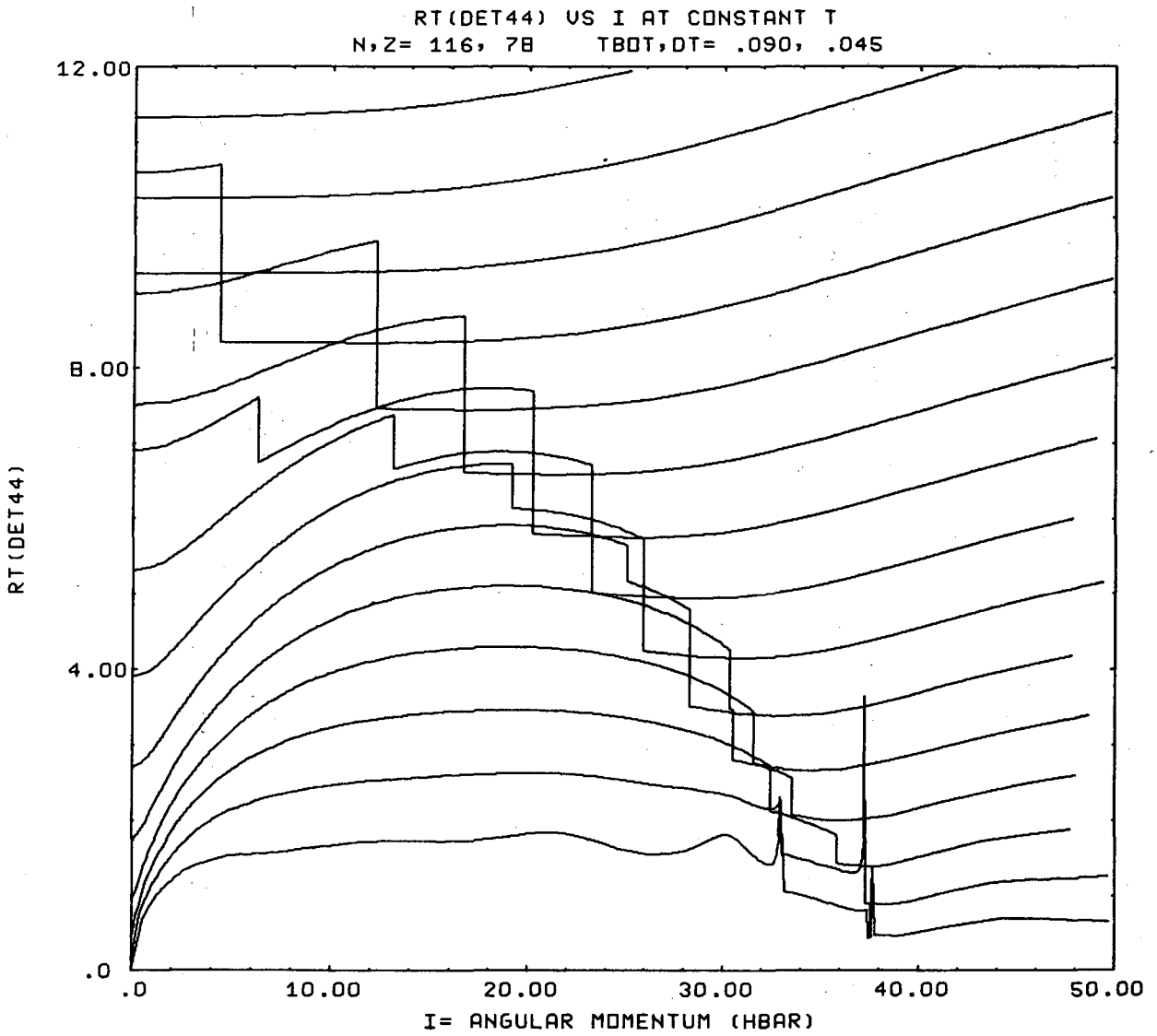

XBL 733-274

Fig. 17

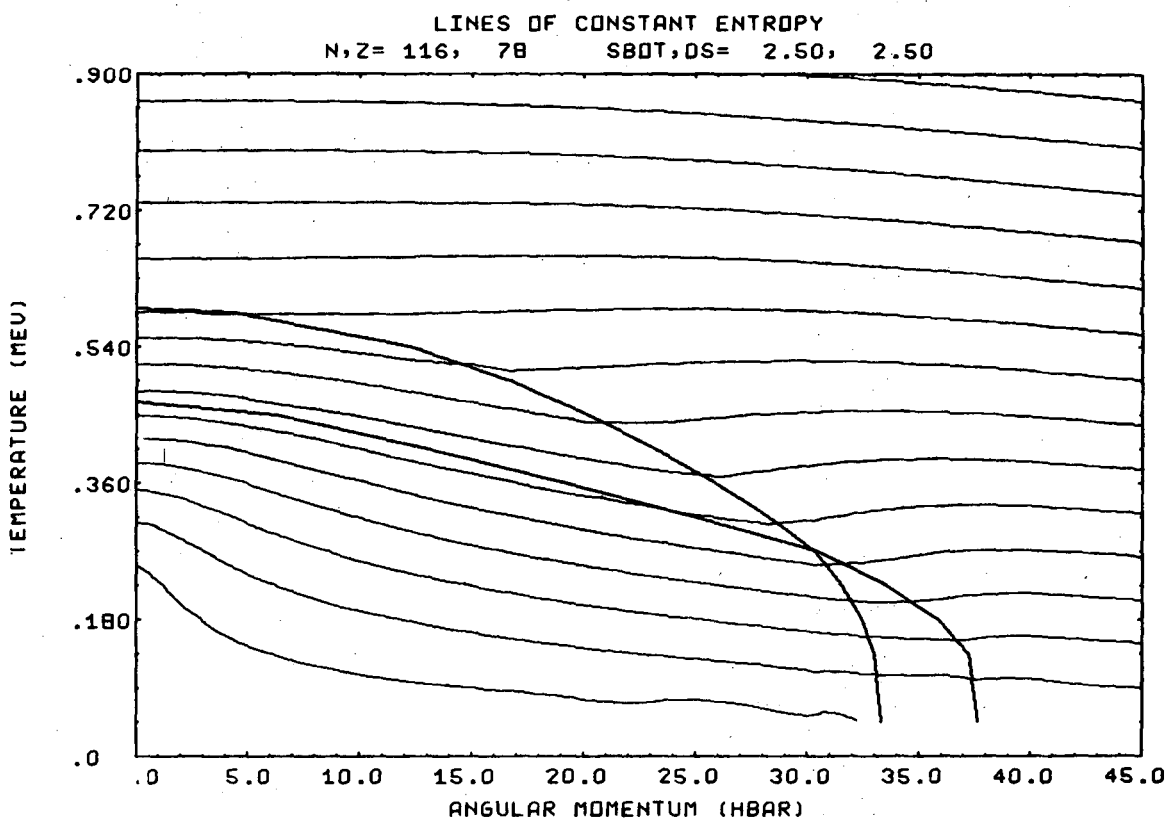

XBL 734-415

Fig. 18a

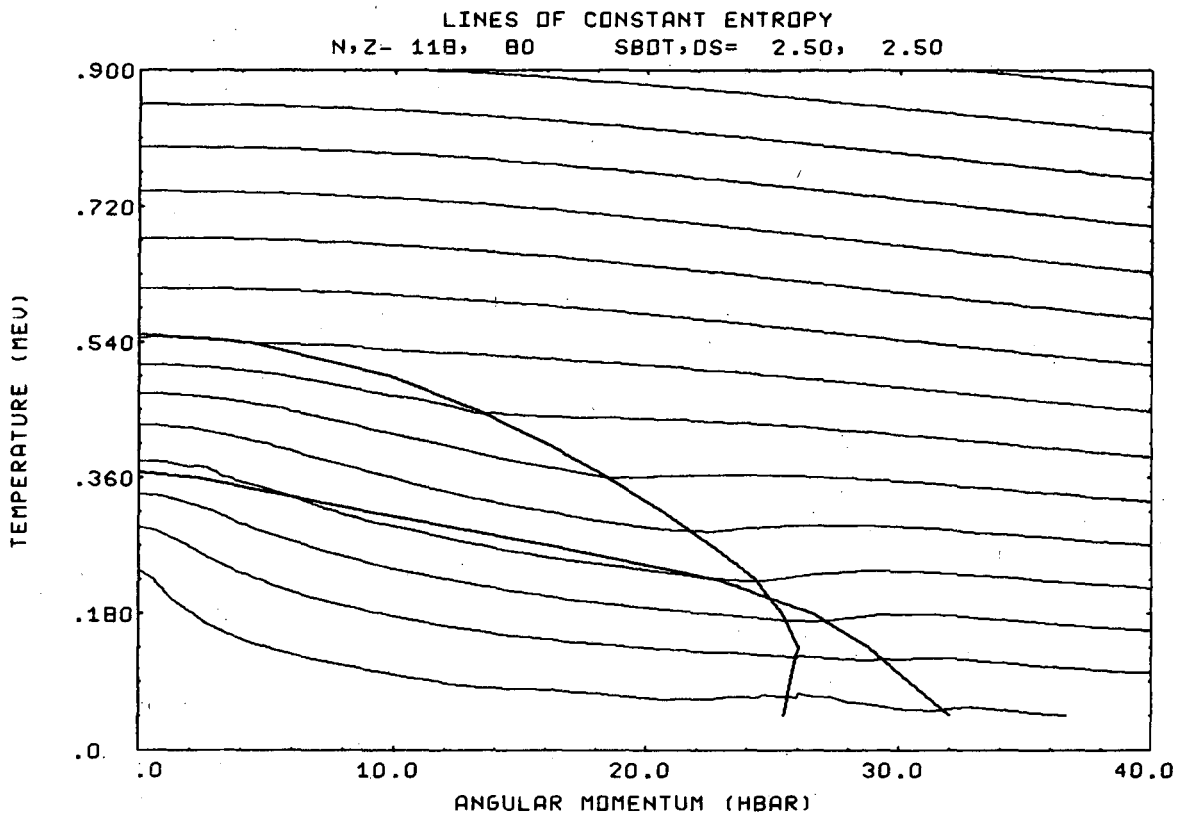

XBL 734-417

Fig. 18b

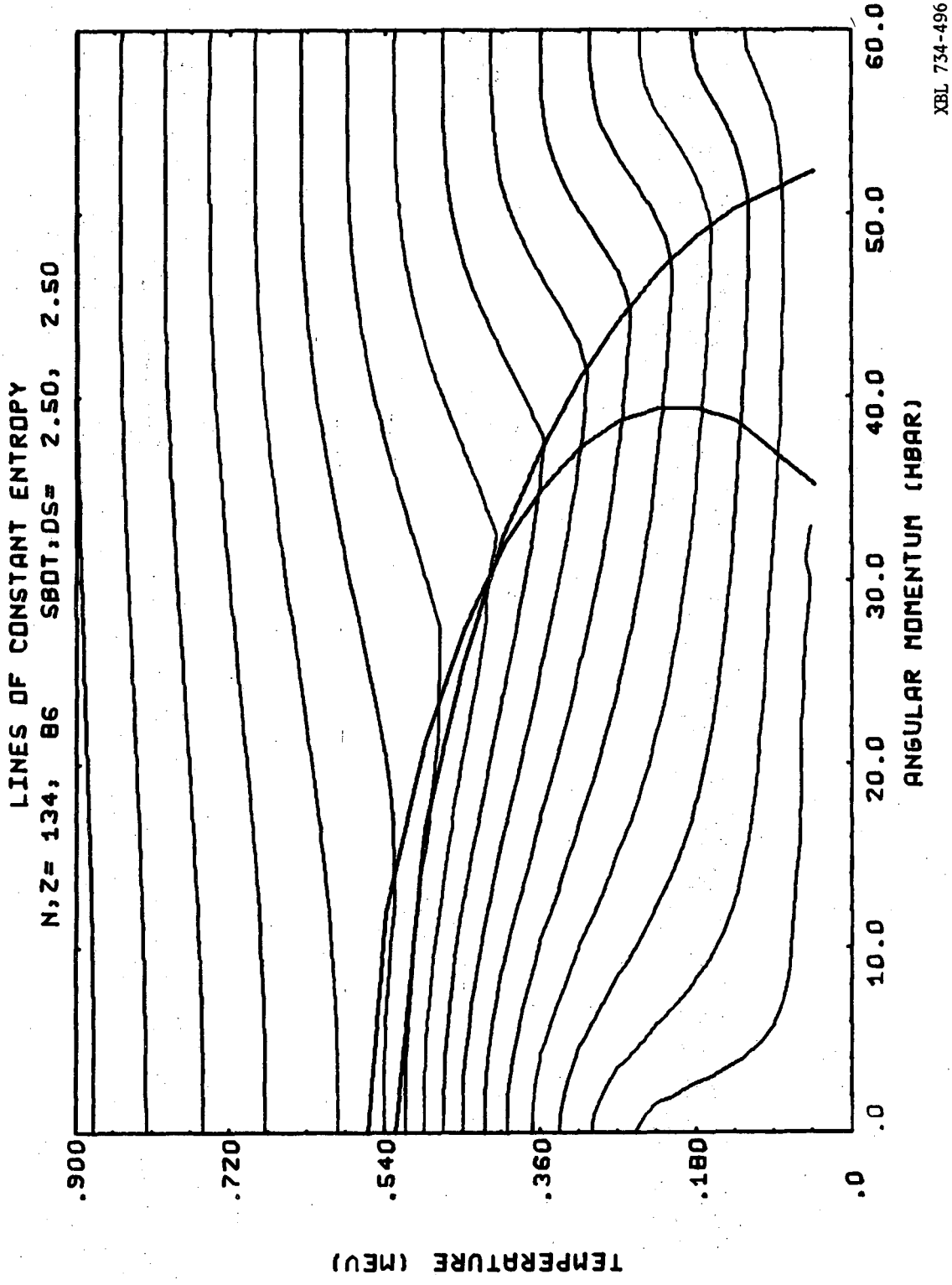

XBL 734-496

Fig. 18c

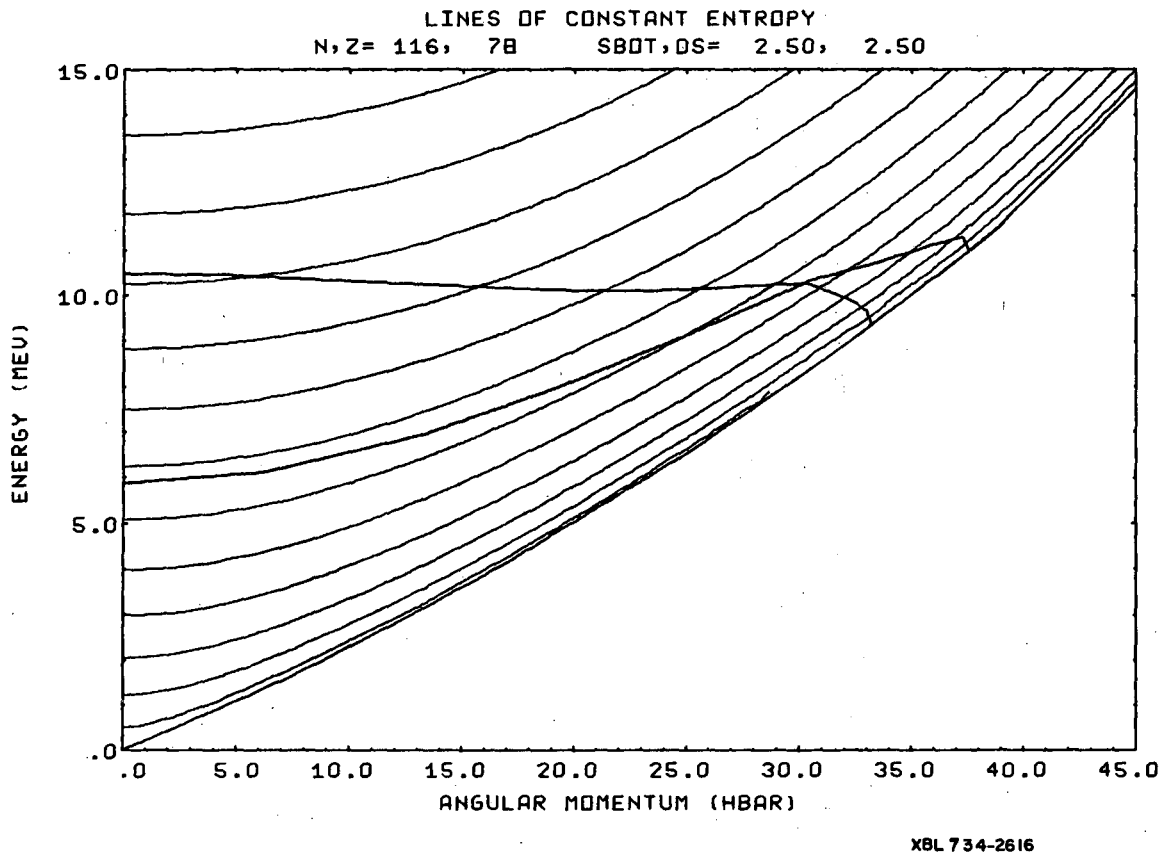
LINES OF CONSTANT ENTROPY
N,Z= 116, 78 SBOT,DS= 2.50, 2.50
15.0
10.0
5.0
.0
ENERGY (MEV)
.0
5.0
10.0
15.0
20.0
25.0
30.0
35.0
40.0
45.0
ANGULAR MOMENTUM (HBAR)
XBL 734-2616

Fig. 19a

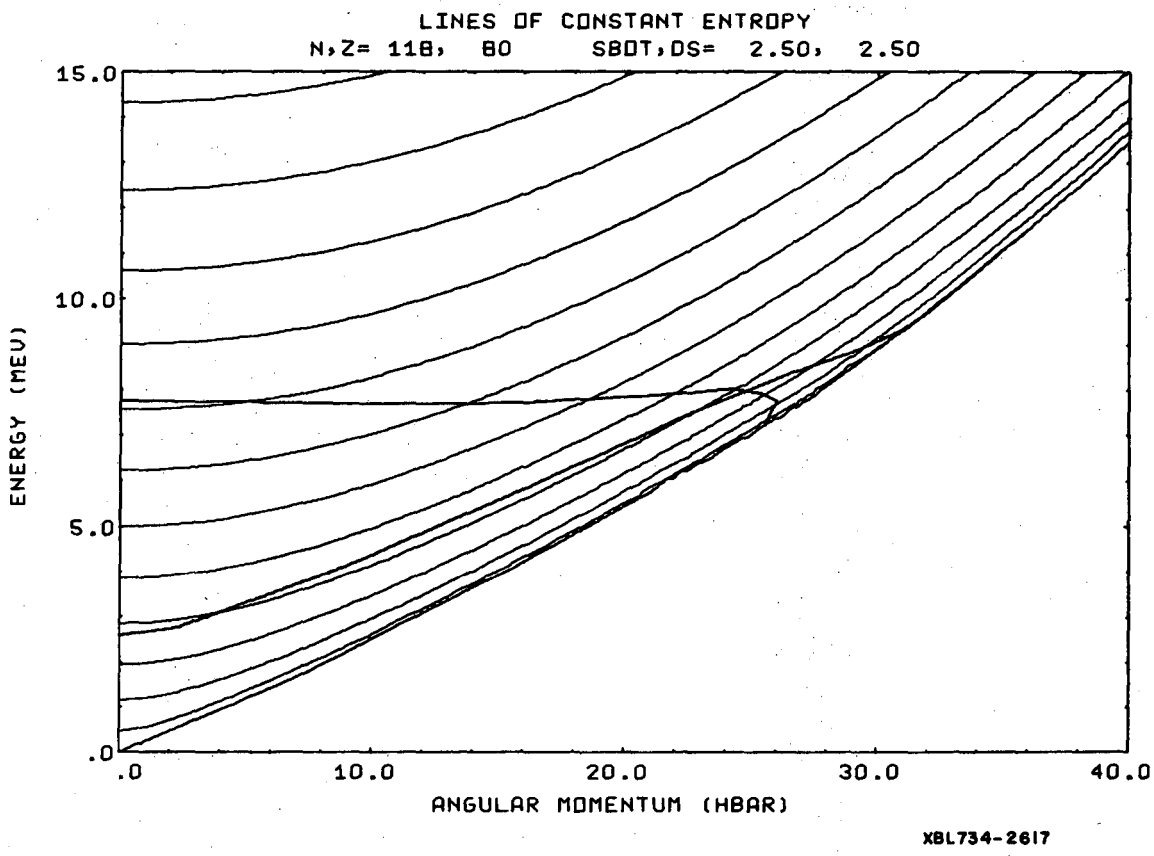
LINES OF CONSTANT ENTROPY
N,Z= 118, 80 SBOT,DS= 2.50, 2.50
15.0
10.0
5.0
.0
ENERGY (MEV)
.0
10.0
20.0
30.0
40.0
ANGULAR MOMENTUM (HBAR)
XBL734-2617

Fig. 19b

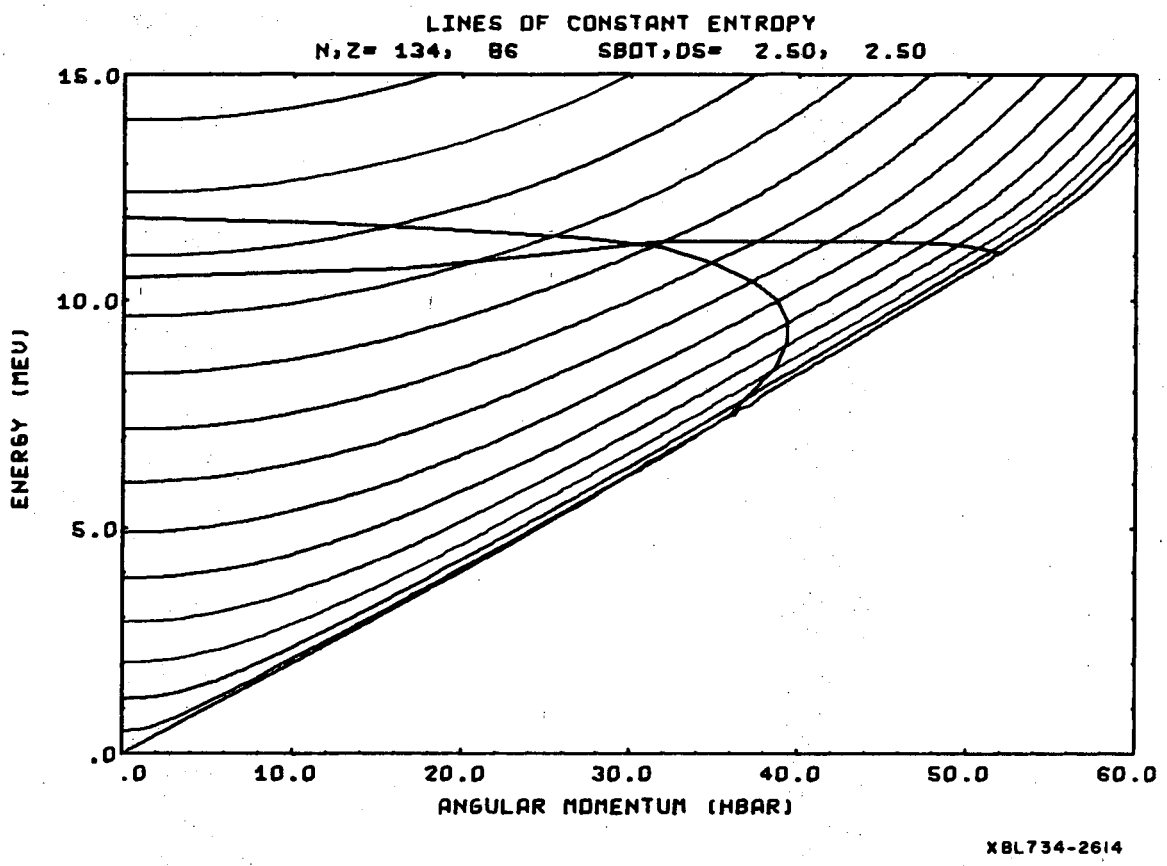
LINES OF CONSTANT ENTROPY
N,Z= 134, 86 SBOT,DS= 2.50, 2.50
15.0
10.0
5.0
.0
ENERGY (MEV)
.0
10.0
20.0
30.0
40.0
50.0
60.0
ANGULAR MOMENTUM (HBAR)
XBL734-2614

Fig. 19c

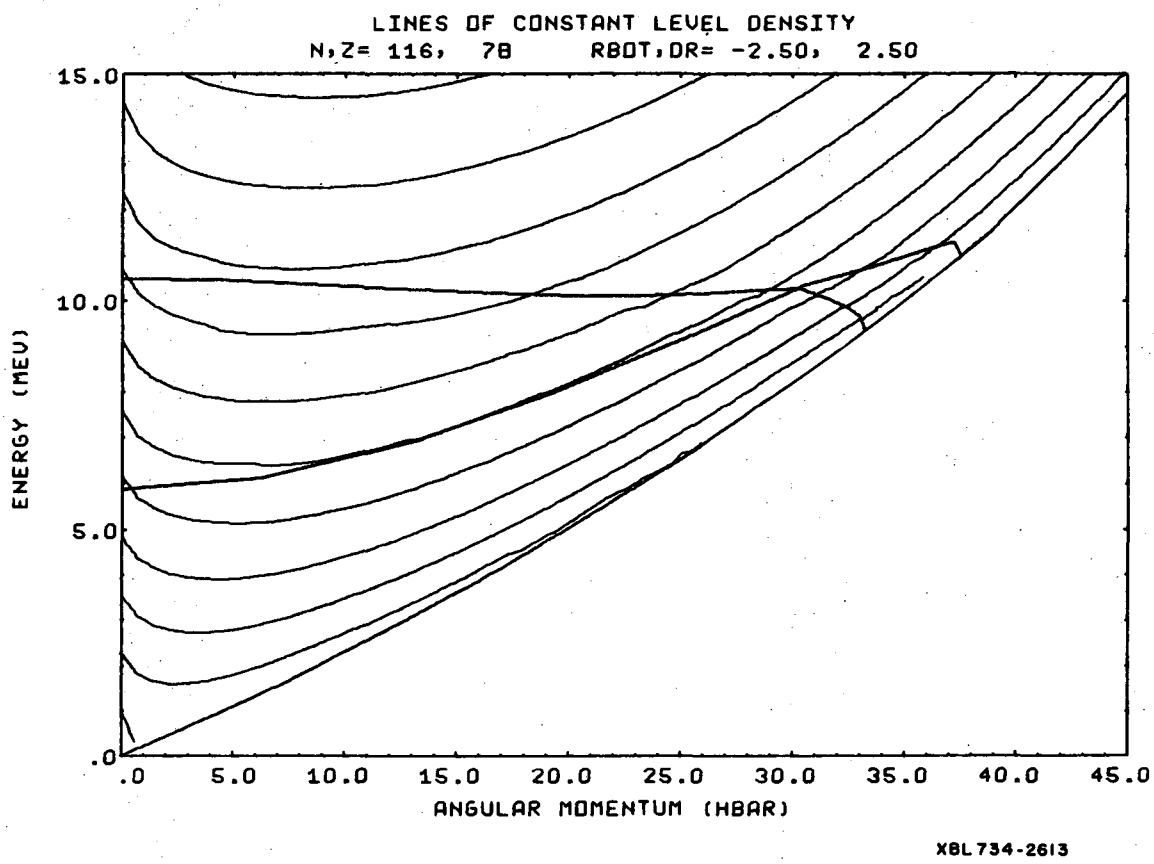
LINES OF CONSTANT LEVEL DENSITY
N,Z= 116, 78 RBOT,DR= -2.50, 2.50
15.0
10.0
5.0
.0
ENERGY (MEV)
.0
5.0
10.0
15.0
20.0
25.0
30.0
35.0
40.0
45.0
ANGULAR MOMENTUM (HBAR)
XBL734-2613

Fig. 20a

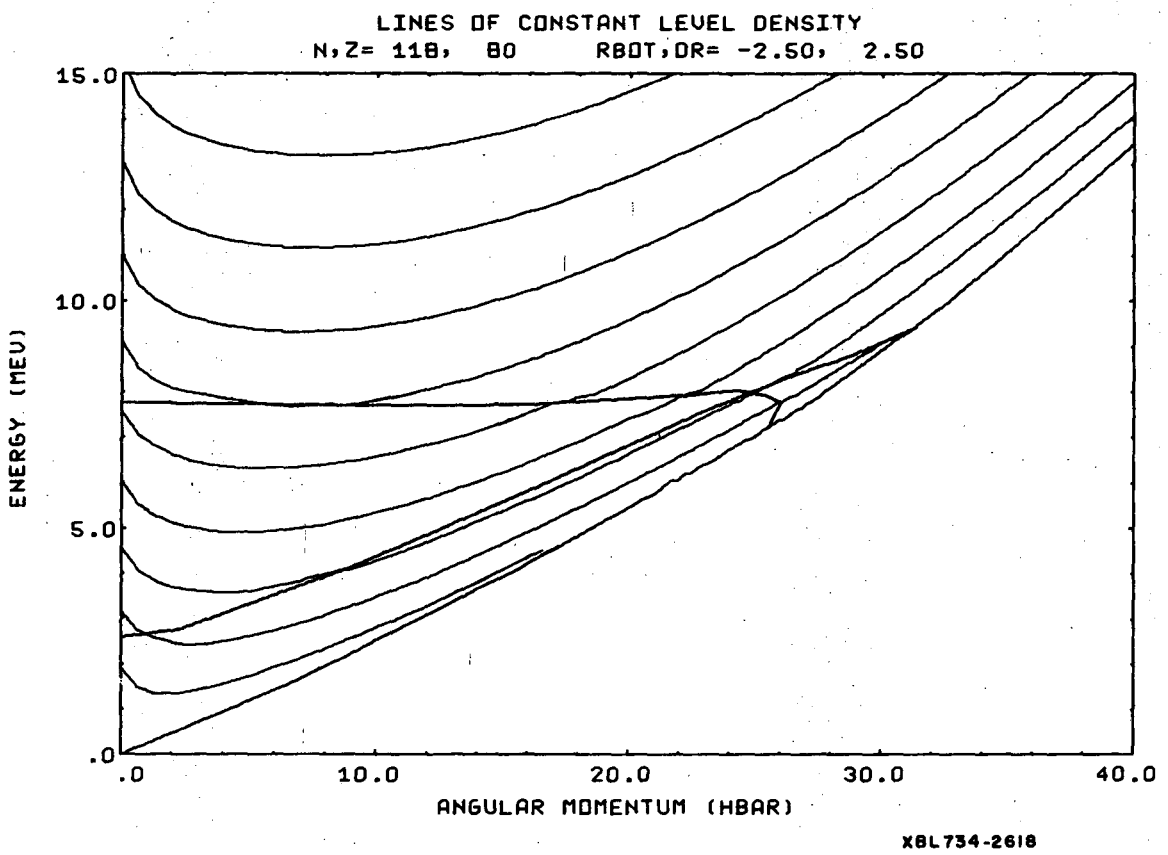
LINES OF CONSTANT LEVEL DENSITY
N,Z= 118, 80 RBOT,DR= -2.50, 2.50
15.0
10.0
5.0
.0
ENERGY (MEV)
.0
10.0
20.0
30.0
40.0
ANGULAR MOMENTUM (HBAR)
XBL734-2618

Fig. 20b

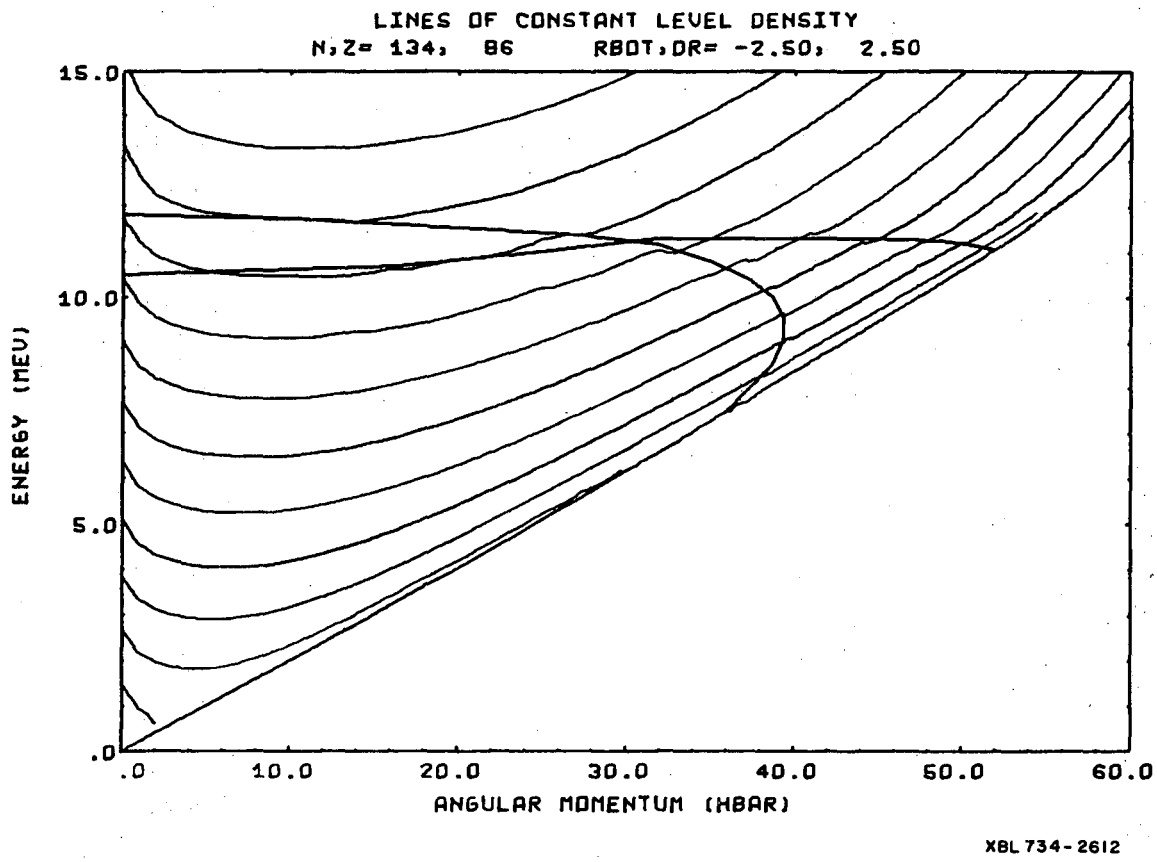
LINES OF CONSTANT LEVEL DENSITY
N,Z= 134, 86 RBOT,DR= -2.50, 2.50
15.0
10.0
5.0
.0
ENERGY (MEV)
.0
10.0
20.0
30.0
40.0
50.0
60.0
ANGULAR MOMENTUM (HBAR)
XBL 734-2612

Fig. 20c

LEGAL NOTICE

This report was prepared as an account of work sponsored by the United States Government. Neither the United States nor the United States Atomic Energy Commission, nor any of their employees, nor any of their contractors, subcontractors, or their employees, makes any warranty, express or implied, or assumes any legal liability or responsibility for the accuracy, completeness or usefulness of any information, apparatus, product or process disclosed, or represents that its use would not infringe privately owned rights.

TECHNICAL INFORMATION DIVISION
LAWRENCE BERKELEY LABORATORY
UNIVERSITY OF CALIFORNIA
BERKELEY, CALIFORNIA 94720